6-1-2014

A method of correction for the effect of optical traps in equilibrium microrheology experiments

ElHassan ElSabry

The American University in Cairo

School of Sciences and Engineering (SSE)

A METHOD OF CORRECTION FOR THE EFFECT OF OPTICAL TRAPS IN EQUILIBRIUM MICRORHEOLOGY EXPERIMENTS

A Thesis Submitted to

The Physics Department

in partial fulfillment of the requirements for

the degree of Master of Science (in Physics)

by ElHassan A. ElSabry

(under the supervision of Dr Karim M. Addas)

May/2014

AChKNOWLEDGEMENTS

All experiments for this research were conducted at the Third Institute of Physics-Biophysics (DPI) at the Georg-August University in Göttingen, Germany. The institute also covered all the costs for the materials and equipment used in the project. I would like to deeply thank Dr. Christoph Schmidt (institute director) for all the time and effort he invested in my guidance and for the help he provided in explaining the findings of the research. He did not hesitate to make all of the institute's resources open for my disposal at any time during my stay.

I would like also to thank Marcel Bremerich (then, PhD candidate at the institute) for the effort he spent in providing me with necessary training on using the experimental setup and for being always available to help in solving different technical difficulties, both with the setup and in the data analysis software.

Special thanks are due to my thesis supervisor, Dr. Karim Addas, Assistant Professor at the AUC Physics Department, for the interest he showed in teaching me, both the knowledge and the skills that allowed me to work on this project. He was patient enough to go through all the details of the work and make sure that I learn how to fix my mistakes and learn from them.

Funds for my travel and accommodation to work on this project were available through the Graduate Student Grant (Office of the Dean of Graduate Studies at AUC) and the generous support of the institute in Germany.

ABSTRACT

University Name: The American University in Cairo

Thesis Title: A method of correction for the effect of optical traps in equilibrium microrheology experiments

Student Full Name: ElHassan Anas ElSabry

Supervised by: Dr. Karim Addas

Optically trapped dielectric particles experience a linear restoring force due to the trapping laser beam for small displacements of the trapped beads from the center of the optical trap. The optical force adds an apparent contribution to the measured shear elastic modulus of the solution in microrheology experiments. Traditional methods of correcting for the effect of the trap and obtaining the true shear elastic modulus of the solution involved taking measurements in separate purely viscous solutions using similar but not identical trapped beads under the same experimental conditions. A new method is proposed in this research to do this correction. It is based on finding the apparent response of the system including solution and trap at two different laser powers then extracting the true medium response from the measured responses. It was found to be an effective method to correct for the optical trap effect for samples of purely viscous solutions that theoretically should have zero elastic shear modulus. It was also tested in a solution of worm-like micelles to check its viability in solutions that have an inherent elastic component of shear modulus. Measurements in water yielded a zero elastic shear modulus and those in micelle solution agreed with previously published data for worm-like micelles solutions. The new method requires less labor and avoids possible sources of error involved in the traditional methods.

TABLE OF CONTENTS

Table of Contents

I. Introduction

"A laser is a solution seeking a problem". So said Theodore Maiman the inventor of the first laser and he was definitely right. Since the firing of the first laser in May 16, 1960, new laser applications never seize to be extremely useful in research and industry. The 1970s was a decade marked by the appearance and development of one of those valuable applications. That is, optical trapping (A. Ashkin 1992).

Optical trapping is a method through which the momentum transfer from laser photons to a nano or micron-sized dielectric object creates forces that can be used to trap that object. Trapping and manipulating of objects, from small molecules, to bacteria, viruses and organelles of eukaryotic cells became possible through optical trapping. Needless to say, this has made it a very essential tool in many fields of research (Neuman and Block 2004). Studying the material properties (viscous and elastic shear modulus) of complex fluids is one such application. By tracking the Brownian motion of micron sized dielectric spheres embedded in the solution under study, the material properties of the solution can be measured (Schnurr, et al. 1997). The laser is the means for both trapping and motion detection. The Fluctuation-Dissipation theorem (explained in the next section) is used to relate the Brownian motion fluctuations to the medium's response. The generalized Stokes-Einstein relation obtains the shear modulus from the response (Schnurr, et al. 1997).

The effect of a laser beam on a trapped spherical dielectric particle is to apply a linear restoring force on the particle for small displacements of the particle from the center of the optical trap. In order to measure the optical force on trapped particles, the trap stiffness must be calculated.

The linear restoring force on trapped particles appears as an apparent contribution to the measured elastic shear modulus (Addas, Schmidt and Tang 2004). If the complex solution under study has itself an elastic component of shear modulus, then it would be necessary to remove the effect of the optical trap in order to obtain the desired properties of the solution under study. Previous methods of measuring the trap stiffness have relied on taking measurements on similar but not identical particles in separate purely viscous

solutions under the same experimental conditions (Addas, Schmidt and Tang 2004) (Neuman and Block 2004). This is to make sure that the measured force is only due to the laser trap. Techniques used to measure the trap stiffness in purely viscous solutions rely on assuming the particle size, solution viscosity and temperature. Furthermore, the solution viscosity can change as the particle gets closer to surfaces and commercially available particles have a certain degree of polydipersity in size (Neuman and Block 2004). For all these reasons, it would be highly desired to develop a method to measure the trap stiffness directly in the solutions under study using the same particles that are used to obtain the materials properties of the solutions. The purpose of this study is to provide such a method.

The method is based on measuring the response of the system (the medium and the optical trap together) at two different laser powers. The true response of the medium can be extracted from the two measured responses and the relative strength of the two laser powers.

The experimental work was divided into two main sections. First, the method was tested in water (which is a medium of a well-known "zero" elasticity). This was done using two particle sizes to make sure the effectiveness of the method was not dependent on particle size. Second, the applicability of the method for viscoelastic media (those that have both viscous and elastic components) was verified through applying it to a solution of wormlike micelles. In both cases, the method was also tried using multiple laser powers (instead of just two) to study if the extracted trap stiffness is any more accurate.

For a comprehensive understanding of the technique proposed by this research, acquaintance with the theoretical basis of two topics is essential. These are the theory optical trapping and microrheology (which is the study of elastic and viscous properties of complex fluids at the micro-scale). The **Background** section below aims to fulfill this purpose by introducing these to fields.

II. Background Information

(1) Optical Trapping

a. Basics

Optical trapping is a technique whereby the force resulting from photon momentum transfer (due to a highly focused laser) to a micron or nano sized dielectric particle can be used to trap this particle.

The trap is created near the focal point of the laser (a little bit downstream on the direction of propagation). It applies a force on the trapped particle analogous to the force of a linear spring and a related stiffness (spring constant) can be defined thereof (A. Ashkin 1992). If the experimental setup allows moving the laser beam, or even moving the stage containing the sample, the optical trap can also be used to manipulate this particle (Neuman and Block 2004).

The theoretical basis for this trapping effect can be understood depending on the size of the trapped object (of radius "r") relative to the wavelength of the trapping laser ("λ") (Neuman and Block 2004).

When $r >> \lambda$, the condition for Mie-scattering applies and the force on the particle can be understood through the application of simple geometrical optics.

When $r << \lambda$, the theoretical treatment is within the Rayleigh-scattering regime. The trapped object then can be viewed as a point dipole.

To illustrate how the optical forces result in successful trapping of particles, the description below will assume the Mie regime. In this context, the description will be through geometrical optics, assuming the following model (Figure 1) where the laser light falls on a dielectric spherical particle as a group of rays. For successful trapping, the particle must be in stable equilibrium in all directions. In this description, the directions of interest are the "*axial*" direction and the "*lateral*" one.

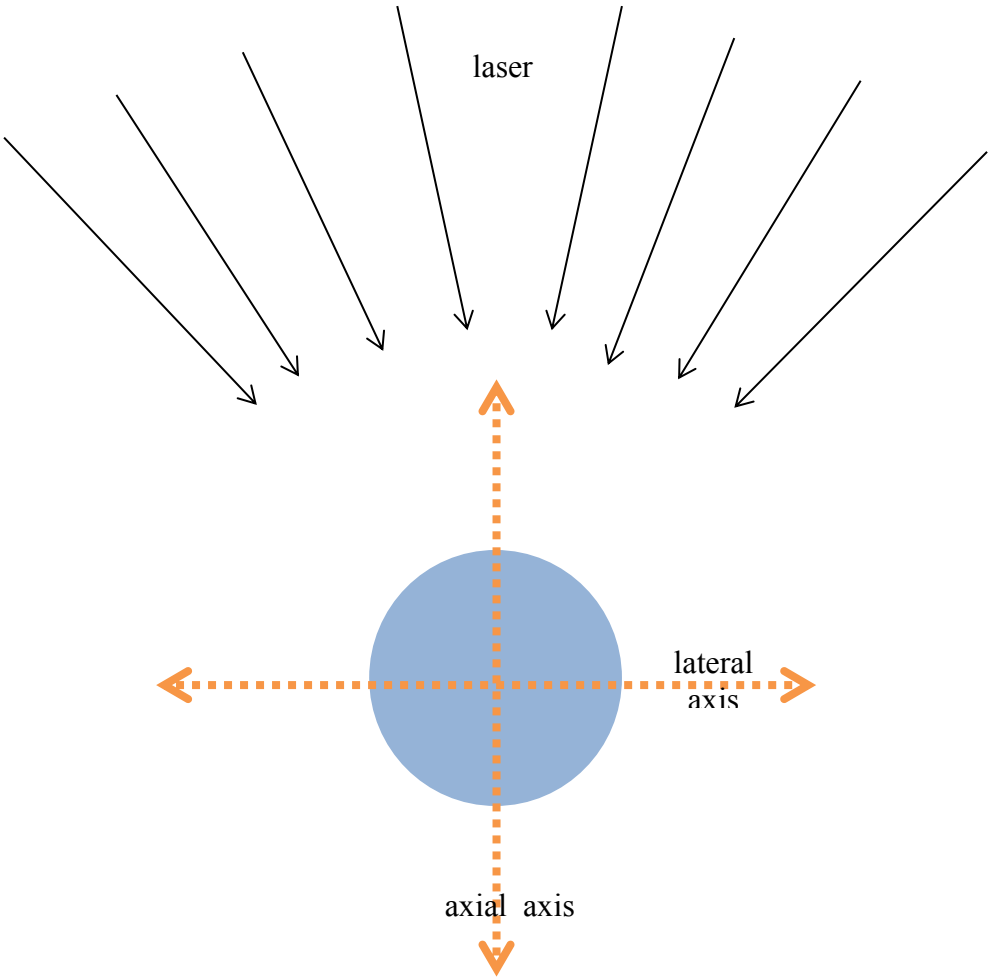

Figure 1: successful trapping of the particle requires that all forces acting on the axial, as well as the lateral, directions are in equilibrium

Along the *axial* direction (Figure 2) there is a very significant force, that is the **scattering force**. It acts in the direction of propagation of light. The origin of this force is the change of momentum of the photons (from the reflected rays) hitting the particle. This force is usually the one that dominates (the same way like water coming out of a hose can push a ball along the direction of flow). However, given the very steep focusing of the light because of the objective's high numerical aperture, the contribution from another force (other than the scattering one) starts to be non-negligible. That is the **gradient force**. It can be attributed to the refracted part of the beam.

As shown in Figure 2, the change in direction of the incident beam (by the time it leaves the particle from the other side) results in a change in momentum. This change in momentum can be represented as force acting on the particle.

The main assumption is that this **gradient force** is proportional to how steep the gradient is and always acts towards the beam's focal point along the *axial* direction.

Therefore, at a certain position along the axial direction, stable equilibrium takes place and causes the particle to be trapped.

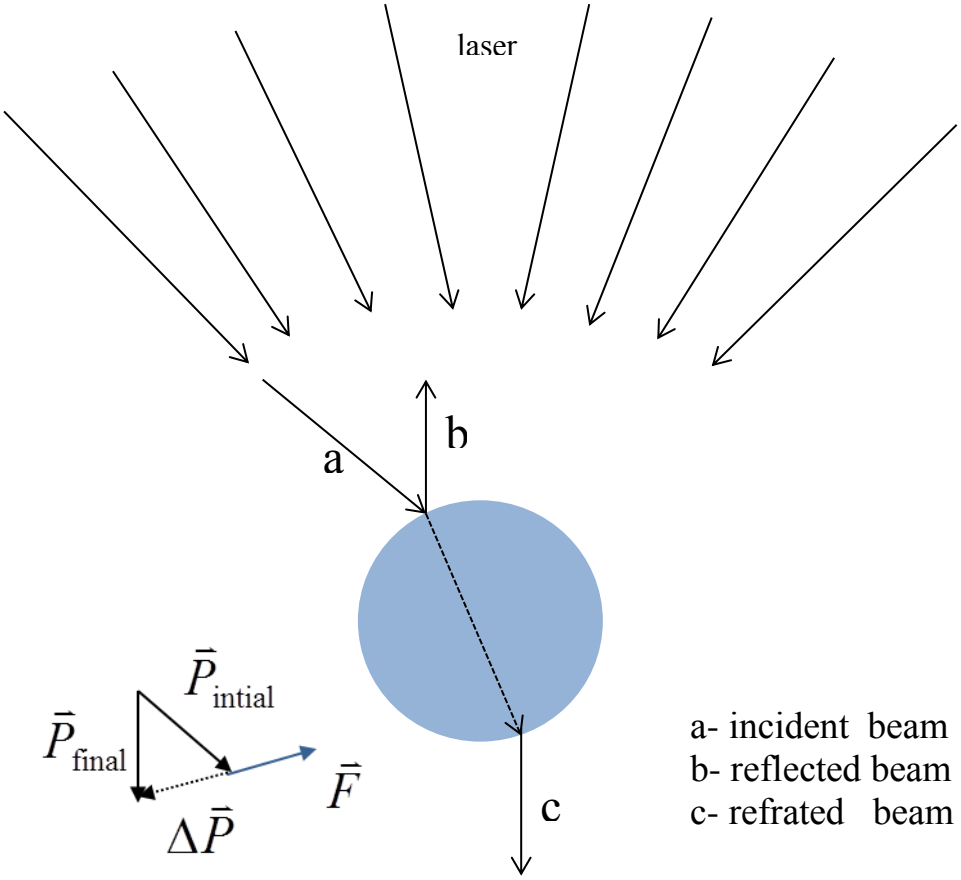

Figure 2: momentum change due to reflected beam's change in direction produces the scattering force (acting downwards) and momentum change due to refreacted beams's change in direction produces the gradient force (acting upwards)

In the *lateral* direction, the Gaussian beam profile plays an essential role in trapping the particle. As shown in Figure 3 below, assuming the particle is a little bit displaced away from the line of maximum intensity in the middle of the Gaussian profile, two rays falling on either side of the particle will be different in intensity (illustrated by ray thickness). Consequently, the two forces resulting from the change in momentum imparted by both rays will also be different. The force resulting from the ray with higher intensity will be larger and will act in a direction that will bring the particle back to the center of the laser beam. Therefore, every time the particle drifts away from the

center of the beam, the gradient force in the *lateral* direction brings it back to the center. This effect, in combination with the effect of stable equilibrium along the *axial* direction, causes the creation of a three-dimensional trap for the dielectric particle.

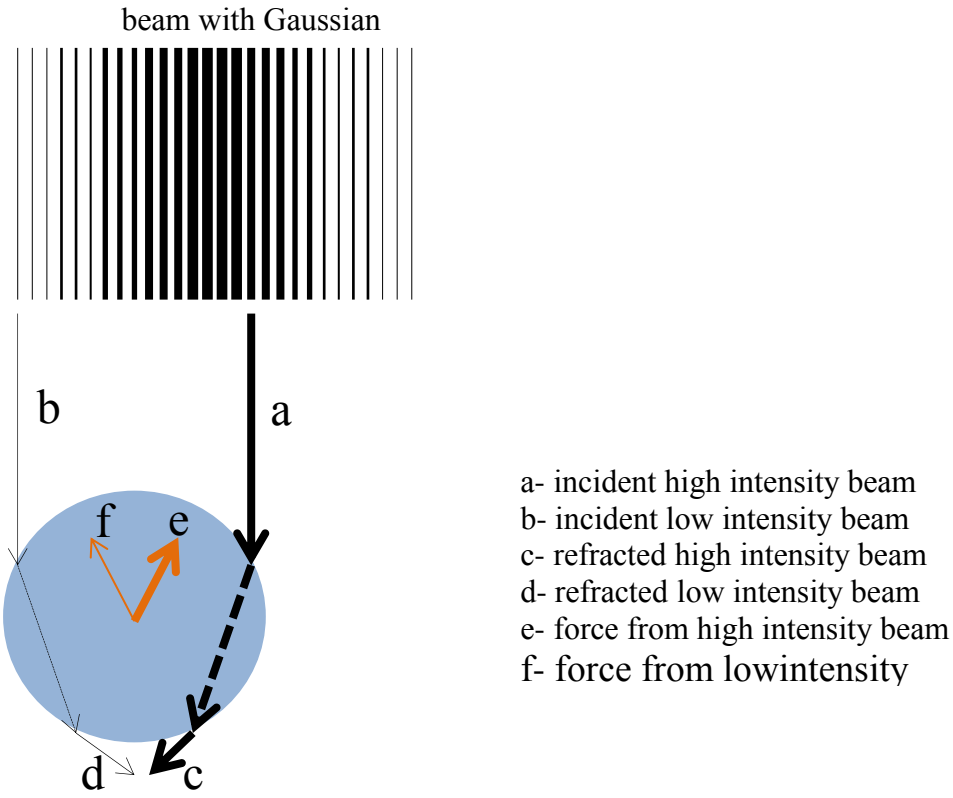

Figure 3: component of (e) along the lateral axis will be larger in magnitude but opposite in direction of that of (f), which leads to the a net force of the particle to bring it back to center of the beam

This mode of optical trapping is known as the "single-beam gradient force optical trap". It came to life in 1986 (Ashkin, et al. 1986) after successful trials of trapping micron-sized particles using more than one laser propagating in opposite directions.

b. Design Considerations

A detailed description of the experimental setup is given below in the EXPERIMENTAL SETUP section. However, here a general listing (Neuman and Block 2004) is given of the some of the important considerations that need to be accounted for in setting up an optical trap.

The main requirement for effective optical trapping is to use a laser beam with a Gaussian profile that overfills the back aperture of a high numerical aperture objective lens. .

A high numerical aperture makes the laser focus very tight and (consequently) the intensity gradient very steep, aiming to maximize the gradient force. It is important to have a large mismatch in index of refraction between the particles to be trapped and the surrounding solution.

A Gaussian beam (in TEM_{00} mode) when focused produces the very high intensity at the center of the beam and lower intensity around it. This makes an intensity gradient towards the center from all lateral directions. This contributes to maximizing trapping efficiency.

If the experiments require the trap to move, suitable steering optics need to be in place. Many options are available for this purpose. The most common are acousto-optic deflectors, electro-optic deflectors and the more traditional scanning mirrors. Other than manipulating the trapped particle, steering optics can also be used to create multiple traps using a single beam. This is easily achieved if the steering optics were rapid enough to change the trap position faster than the Brownian relaxation of the trapped objects.

The optical trap is usually incorporated into a custom built or commercially available microscope to be able to view the sample while trapping.

(2) Microrheology

a. Basics

Rheology is the study of the deformation and flow of matter. In other words, it examines the elastic and viscous properties of different materials on a macroscopic level. The discipline of *microrheology* on the other hand refers to such studies when they are done on the micro-scale. Its focus is on the "local" viscoelastic properties of materials. Materials like polymer solutions, gels and protein filament networks (all referred to as soft matter) are usually studied using microrheological techniques. These materials exhibit a very interesting phenomenon, which is the significant dependence of their shear modulus on frequency (with corresponding time ranges of milliseconds and seconds, even minutes in some cases) (MacKintosh and Schmidt 1999). The quantity of

interest in microrheological experiments is usually the dynamic shear modulus ‘’G’’.

Consider the application of a shearing force (parallel to the surface) on a given body (Figure 4). This force will cause deformation in the body shape and the stress in this case will be defined as $\sigma(t) = \frac{F(t)}{A}$. The measure of deformation of the shape of that body will be called strain and defined by the angle $\gamma(t) = \frac{x(t)}{h}$ (for small angles such that $\tan(\gamma) \sim \gamma$).

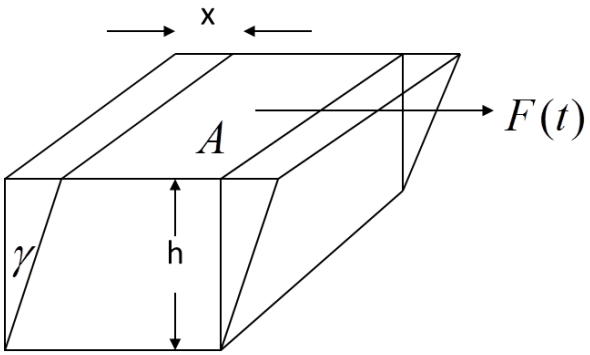

Figure 4: body under stress exhibiting some strain

For a periodic strain of the form $\gamma(t) = \gamma_o \sin(\omega t)$, the stress takes the form $\sigma(t) = \gamma_o G' \sin(\omega t) + \gamma_o G'' \cos(\omega t)$. If the body is perfectly elastic, the stress will be in phase with the strain and only the first term in the previous expression will exist. For a purely viscous medium, the stress will be 90 degrees out of phase with the Strain. In this case, only the second term will exist. The third case would be if the body is a combination of both (i.e. a viscoelastic solution). In this special case, part of the applied stress will be in phase with the strain and another part will be out of phase with it. The coefficient of the first part will constitute the elastic component of the shear modulus (G') and that of the second part will constitute the viscous component of the shear modulus (G''). The dynamic shear modulus (mentioned above) will be defined as a complex quantity $G(\omega) = G'(\omega) + iG''(\omega)$ whose real part represents the contribution of the elastic part of the solution (e.g. the polymer network) to its response to periodic stress and its imaginary part represents the contribution to response from the viscous component.

Several techniques were developed to study material properties at the micron-scale (MacKintosh and Schmidt 1999). Among these techniques is the measurement done using micron-sized probe particles. This involves introducing probe particles to the solution under study and measuring the Brownian motion of the probe particles. In this research, single spherical silica particles, about one micron in diameter, are trapped using a laser beam as discussed in the previous section.

b. Correction for the Trapping Force Effect

The Langevin equation applied to a particle trapped in a purely viscous solution and has the following form

$$m\ddot{x}(t) = \xi(t) - \gamma\dot{x}(t) - \kappa\, x(t) \qquad (1)$$

where $\xi(t)$ is the random Brownian force acting on the particle resulting from the collisions of the solution molecules with the particle. The term $-\gamma\dot{x}(t)$ is the viscous force of the solution acting on the particle. The laser force acting on the particle can be modeled by a linear restoring force $-\kappa\, x(t)$. In the frequency domain (after performing a Fourier transform), the Langevin equation has the form

$$-m\omega^2 x(\omega) = \xi(\omega) - i\omega\gamma\, x(\omega) - \kappa\, x(\omega) \qquad (2)$$

The "response" of the system is defined through the relation (displacement = response x external force). Taking the external force on the particle to be only the Brownian force,

$$x(\omega) = \left[\frac{1}{\kappa - m\omega^2 + i\omega\gamma}\right] \xi(\omega) \qquad (3)$$

The response can be identified from the previous equation as

$$A(\omega) = \frac{1}{\kappa - m\omega^2 + i\omega\gamma} \qquad (4)$$

The complex shear modulus is related to the complex response of the system through the generalized Stokes Einstein relation (Schnurr, et al. 1997).

$$G(\omega) = \frac{1}{6\pi r\, A(\omega)} \qquad (5)$$

where r is the radius of the particle. For the response of Equation-4, we get a complex shear modulus

$$G(\omega) = \frac{\kappa - m\omega^2 + i\omega\gamma}{6\pi r} \tag{6}$$

ignoring the inertial term which only becomes significant at very high frequencies, we get a shear modulus of the form

$$G(\omega) = \frac{\kappa}{6\pi r} + \frac{i\omega\gamma}{6\pi r} \tag{7}$$

As mentioned in the previous section, the complex shear modulus of the system takes the form

$$G(\omega) = G'(\omega) + iG''(\omega) \tag{8}$$

where $G'(\omega)$ is the storage modulus (elastic component) and $G''(\omega)$ is the loss modulus (viscous component).

The first term in Equation-7 describes an apparent elastic modulus due to the presence of the optical trap. The central idea of the thesis is how to remove this apparent term in order to obtain the true shear modulus of the solution.

If we consider the external force on the particle to be the sum of the Brownian force and the trapping force, we have

$$x(\omega) = \left[\frac{1}{-m\omega^2 + i\omega\gamma}\right][\xi(\omega) - \kappa\, x(\omega)] \tag{9}$$

The response in this case can be identified as

$$\alpha(\omega) = \frac{1}{-m\omega^2 + i\omega\gamma} \tag{10}$$

The shear modulus (ignoring the inertial term) obtained from the response $\alpha(\omega)$ is

$$G(\omega) = \frac{i\omega\gamma}{6\pi r} \tag{11}$$

which represents the true shear modulus of the medium without the effect of the optical trap.

Due to the previous analysis, the response α(ω) will be denoted as the true response of the solution and $A(\omega)$ will be denoted as the apparent response which includes the effect of the optical trap. The relation between the two responses can be obtained from Equations-4 and 10

$$\alpha(\omega) = \frac{A(\omega)}{1 - \kappa\, A(\omega)} \tag{12}$$

The response that is measured in experiments is the apparent response $A(\omega)$. Equation-12 then relates the apparent response to the true response of the solution α(ω). The trap correction process then involves the measurement of κ in order to use (along with the measured apparent response) to calculate the true response of the solution.

III. Literature Review

As mentioned, it is necessary to ensure that the response produced during microrheological experiments is only a result of the viscoelastic properties of the medium under investigation and not an apparent effect due to the trapping laser. Because of the large amount of variables (related to the environment in which the measurement is taken), this trap correction process remains largely experimental in the current microrheological research projects.

There are several methods that are used in the literature to correct for the trap effects (Neuman and Block 2004) (Marti and Hübner 2010). Below is a listing of the most common methods and a brief description of each one. It is important to note that the discussion below is limited to methods that determine the lateral components of the trapping force, not the axial one.

The common methods to calculate the stiffness of the trap can be categorized to three types. Method "1" offers a way to *directly* measure the force on the particle from the laser. Method "2" is based on calibrating the trapping force against another known one. The rest of the methods (Method "3" to "5") are statistical in nature. They use recorded data from Brownian motion of the trapped particle. The data is then fitted to a model, the parameters of which include the trap stiffness.

(1) Method "1": Momentum Transfer Method

When the laser light interacts with a trapped particle, the exiting light will experience a change in momentum. The change in momentum of the light results in a force being applied to the trapped particle. By measuring the deflection of the light, the force imparted to the particle can be calculated using the formula $F = \frac{P_s}{c}(\frac{x_{bfp}}{f})$, where P_s is the power of the laser beam in the sample, x_{bfp} is the center of mass of the optical power in the back-focal plane

of the condenser lens, f is the focal length of the condenser lens, c is the speed of light. This method has been demonstrated for a dual-beam optical trap setup (Smith, Cui and Bustamante 2003). Their experiments used low numerical aperture (NA) beams in high NA lenses in order to capture all the laser light that interacts with the trapped particle. Since low NA beams were used, the gradient force was not strong enough to trap the particles. Counter-propagating beams were needed to counter the scattering force on the particles and apply twice the gradient force on trapped particles.

(2) Method "2": Calibration against Drag Force

By generating a relative motion between a trapped particle and the viscous medium around it, a viscous drag force will be applied to the particle. The relative motion is typically induced by moving the whole sample using a piezostage or applying a flow in the chamber. By measuring the position of the trapped particle from the center of the trap in response to the applied drag force and comparing with the theoretical prediction, the trap stiffness can be extracted.

The ability of this method to generate accurate results is restricted by its dependence on the viscosity of the medium (which in turn depends on temperature at that instant and surface proximity effects). This dependence is a source of significant error unless it is corrected for.

(3) Method "3": Using the Equipartition Theorem

The Equipartition theorem relates the average energy per degree of freedom (for quadratic energy terms) to the temperature of the medium. Assuming a harmonic potential for a trapped particle we get $\frac{1}{2}k_{trap}\,\langle x^2\rangle = \frac{1}{2}k_B T$, where k_{trap} is the trap stiffness, k_B is Boltzmann's constant and T is the absolute temperature of the solution. Hence, it is possible to calculate the trap stiffness given a sufficient amount of data for the trapped particle position variance.

This is generally a good method but it is very sensitive to drifts if they exist in the medium where the particle is trapped. Systematic drifting in the particle's position, as well as noise, will influence the position variance causing inaccuracy in the stiffness values obtained.

(4) Method "4": Using the Boltzmann distribution

The probability distribution of the position of a trapped particle is determined by the Boltzmann distribution $P(x) \propto e^{-\frac{U(x)}{k_B T}}$, where $U(x) = \frac{1}{2} k_{trap}\, x^2$ is the potential energy.

The main limitation to this method is that it requires huge amounts of data in order to make sure that the tails of the Gaussian (which include the most of the information about the potential) have enough counts to guarantee accurate results.

(5) Method "5": Fitting Power Spectral Density to a Lorentzian Curve

Among the most common methods involves fitting the power spectral density (PSD) of the random position fluctuations of a trapped particle in a purely viscous solution to a theoretically predicted formula. The theoretical formula is derived from the Langevin equation applied to the trapped particle. The forces acting on a trapped particle are the resultant of three contributions, the thermal force (Brownian motion), the medium friction force and the laser optical force.

In a purely viscous medium of known viscosity, the power spectrum (in the x-direction) for the thermal fluctuations of a trapped particle of radius "r" has a Lorentzian form given by the equation $S_{xx}(f) = \frac{k_B T}{\pi^2 \gamma (f_o^2 + f^2)}$, where T is the absolute temperature, k_B is the Boltzmann constant and $\gamma = 6\pi\,\eta r$ is the Stokes drag coefficient of the particle in a medium of viscosity η.

By fitting the measured PSD data to the Lorentzian curve, the corner (roll-off) frequency $f_o = \frac{k_{trap}}{2\pi\,\gamma}$ can be determined from the curve and using its value, the trap stiffness k_{trap} can be calculated.

As obvious from above, this method requires that the medium viscosity be known. It is also characterized by the ability to calculate the force in the axial direction in case it was possible to record the position fluctuations in that direction. Also, for a method like this one, the signal detection system comes into play with a very important role. A sufficient bandwidth should be

available to generate a good PSD curve that extends for a sufficient range on both sides of the corner frequency.

All of the above methods then suggest that, in using the optical tweezers to determine the shear modulus of a viscoelastic medium, the measurement has to be repeated again in a purely viscous one. In addition, changing the sample can be associated with a wide range of possibilities for experimental error.

The purpose of this research is to propose a new method of correction for the effect of an optical trap using the same particles that are used to measure the material properties, in the same solutions under study, without the need to make separate measurements in different solutions. The following section offers a detailed description of this new method.

IV. Suggested Method for Trap Correction

The method proposed in this thesis for obtaining the true response of a solution involves measuring the apparent response of the system at two different laser powers and extracting the true response of the solution from the measured responses. The apparent responses of the system that include the effects of laser traps of stiffness (κ) and (κ + a κ) will be denoted by β(ω) and $\phi(\omega)$ respectively. The parameter "a" is obtained experimentally by measuring the optical power of the laser beam at two power settings. Since the laser power is linearly related to the trap stiffness, the parameter is calculated as$a = \frac{P_2 - P_1}{P_1}$, where P_1 and P_2 are thelow and high powers , respectively. The correlation between the laser power used and the trap stiffness in the sample was checked and the linear relation can be seen in Figure 5 below.

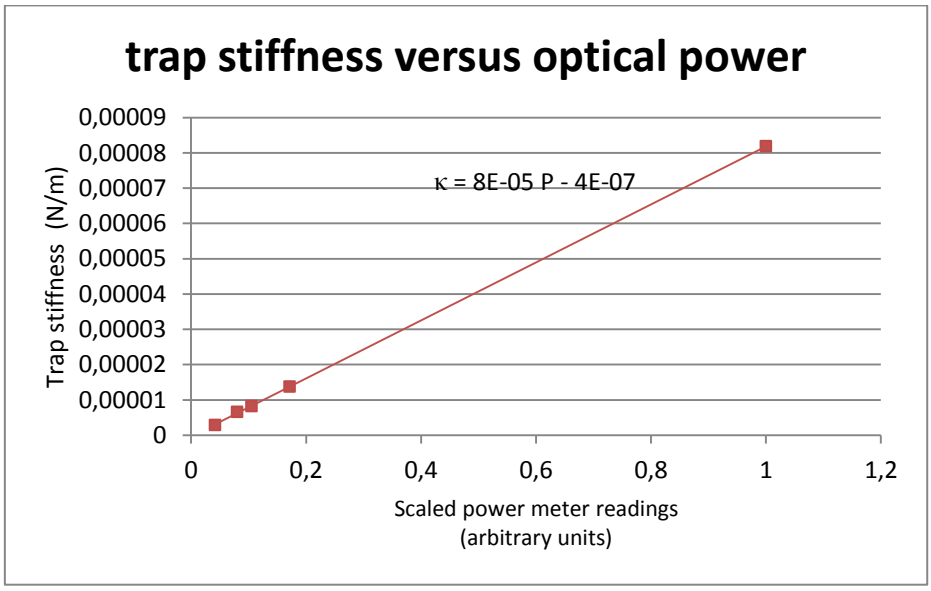

Figure 5: correlation between laser power used and optical trap stiffness

The relation between the apparent response at low power β(ω) and the true response $\alpha(\omega)$ can be obtained from Equation-12

$$\alpha(\omega) = \frac{\beta(\omega)}{1 - \kappa\,\beta(\omega)} \tag{13}$$

Similarly the expression that relates the apparent response at high power $\phi(\omega)$ and true response $\alpha(\omega)$ is also given by Equation-12

$$\alpha(\omega) = \frac{\phi(\omega)}{1 - (\kappa + a\kappa)\,\phi(\omega)} \tag{14}$$

Eliminating the trap stiffness in the two equations gives an expression for the true response of the solution in terms of the responses at the two different laser powers

$$\alpha(\omega) = \frac{a\ \beta(\omega)\ \phi(\omega)}{(a+1)\ \phi(\omega) - \beta(\omega)} \tag{15}$$

Equation-15 is the central result that is tested in this thesis.

V. Experimental Verification

(1) Experimental Setup

A custom-built inverted microscope (Figure 6) equipped with an optical trap is used in the measurements. Real pictures of the setup can be viewed in APPENDIX #3: Experimental Setup Pictures.

As a source of light, a linearly polarized near infrared laser (Compass, ND:YV04, 1064 nm, 4 W, Coherent Inc., Santa Clara, CA) was used. To enhance the stability of the beam, protection against back reflections was provided by an optical isolator (IO-5-1064-VHP, Thorlabs, Newton, NJ, USA). Because of the need to overfill the back aperture of the objective, a beam expander (Qioptiq Photonics GmbH & Co KG, München, Germany) was used. It increased the beam diameter to 4 mm. Then, a combination of a half-wave plate[1] and a Glan-laser polarizer (Thorlabs, Newton, NJ, USA) was put in place to adjust the beam intensity while operating the laser source at maximum power (2 Watt). The setup was originally prepared to make two traps out of the same source. Therefore, a 90^{o} Glan-laser polarizing beam splitter (Artifex Engineering, Emden, Germany) was introduced to split the beam into two[2] orthogonally polarized beams. To steer the reflected beam, acousto-optical deflectors (AOD) (DTSXY-400, AA optoelectronic, Orsay Cedex, France) were available for two dimensions (both in a plane parallel to that of the sample). For coarse motion, two telescope lenses (Thorlabs, Newton, NJ, USA) were used, which also expanded the beam after the AODs.

Through a dichroic mirror (no.1), the beam enters the vertical path where the sample is placed on a piezostage (P561.3CD, 100 _m3, 0.8nm resolution, Physik Instrumente GmbH, Karlsruhe, Germany) to provide computer-controlled high-precision sample positioning in three dimensions.

[1] this half-wave plate was the one used to change laser power for the purpose of this research
[2] beam used in the measurements was the one reflected at the splitter while the transmitted beam was blocked by a shutter placed right after the splitter

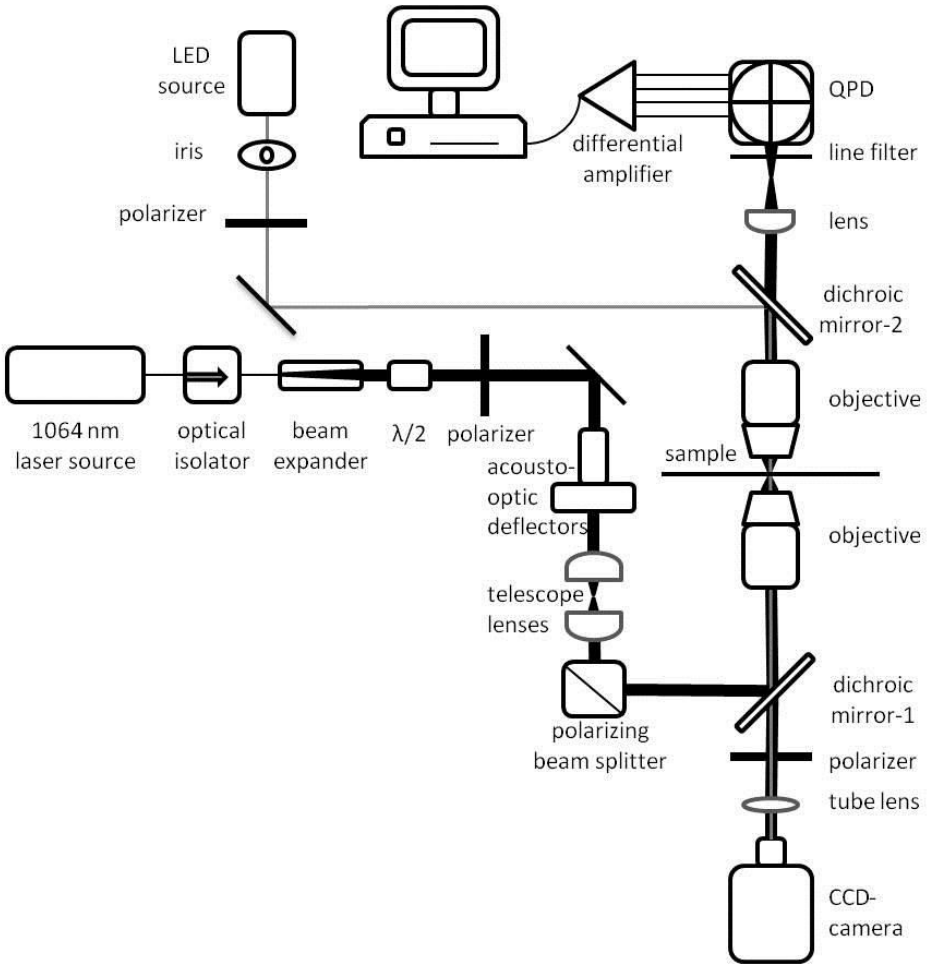

Figure 6: schematic for the experimental setup

Along this vertical path, the beam passes through the following components. First, oil-immersion, infinity-corrected alpha Plan-Apochromat objective (Carl Zeiss, Germany), which has the magnification of 100x and a high numerical aperture of 1.46 to create the steep gradient and hence the optical trap. After the beam leaves the sample chamber, another objective (same as the first one) acts as a condenser. At 2f-distance from the condenser's back focal plane, NIR-antireflection coated 50mm achromatic doublets (AC254-050-B, Thorlabs, Newton, NJ, USA) are put in place to image the back focal plane of the condenser on the QPD. An Nd:YAG enhanced silicon QPD (10mm diameter, SPOT9-YAG, OSI Optoelectronics, Hawthorne, CA, USA) was used to detect laser position fluctuations. It operated under a reverse bias voltage of 160V. To prevent all other light sources from reaching the QPD, a line filter for the 1064 nm wavelength was put right at the QPD entrance point.

The illumination of the microscope was through an LED source and entered the vertical path through another dichroic mirror (no.2).

Data collection from the experiment took two forms. First, the displacement signals were sampled with an FPGA A/D board (NI PXI-7833R, National Instruments, Austin, TX, USA) and processed by custom-written LabVIEW data acquisition software (National Instruments). The recorded position fluctuation data was then processed off-line in MATLAB. Second, to collect the actual sample images a CCD-camera (Cool-Snap EZ, Photometrics, Tucson, AZ, USA) is used. It is placed at the focal length of a tube lens (tube lens 25, Carl Zeiss MicroImaging GmbH, Germany).

It is important to note that several measures were taken in order to minimize the effect from possible sources of experimental noise. For each of these four sources, the following measures were taken.

Mechanical Vibrations: The setup was stationed on top of a passive air table for mechanical isolation.

Temperature Changes: The room temperature was controlled at 21.4° C.

Air Convection: It was made sure that as much as possible of the optical components were enclosed. The air inside the room was also filtered to avoid interruption of the beam by dust particles.

Acoustical Noise: The room was isolated from outside sources of noise. Optical components were also made sure to be very rigid in their attachment to the table. The setup was incorporated in a closed box to eliminate air currents and acoustic vibrations

Appendix #3 includes real pictures of the experimental setup.

(2) Calibration Process

Detecting the motion of the probe particle was performed using a Quadrant Photodiode (QPD). The QPD is sensitive to the laser intensity. Its photocell produces a specific amount of current which corresponds to the amount of light falling on each of the four quadrants. The current is converted to a voltage and is amplified. The calibration factor that converts the QPD voltage to displacement is essential to express particle position in units of meters. This

research did not suggest any new method for getting the position calibration factor. It uses the technique introduced in (Vermeulen, et al. 2006). In this paper, it was argued that the calibration factors converting units of volts to that of position can be obtained by scanning the laser beam (using an acousto optic deflector (AOD) across the particle fast enough to prevent the particle from responding to the optical force of the beam and simultaneously recording the QPD signal. Part of this calibration process was done once. That is calculating the conversion factor between V_{AOD} and the actual particle position in micrometers. Then, for each particle used, a conversion factor was obtained to relate V_{AOD} to the V_{QPD}, eventually producing a factor to calibrate QPD voltage data for each measurement and have them expressed in nanometers to allow for further physical calculations.

The first step was to obtain a conversion factor between V_{AOD} and the relative displacement of the particle center in computer screen pixels. Two trap positions were created using one laser beam oscillating at a high frequency between both positions. This was done by varying the amplitude of the AC signal given to the AOD and measuring distance between the two positions of a double trap on the camera image. Figure 7 shows two particles trapped at two different positions using the same beam.

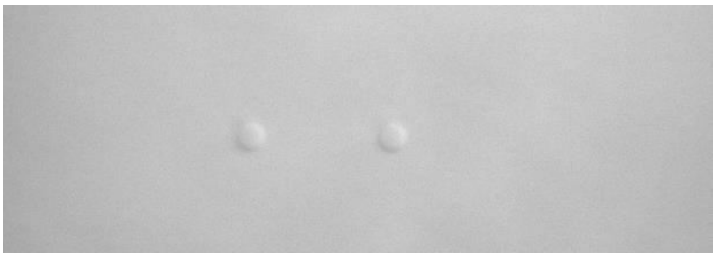

Figure 7: two particle trapped using only one laser beam

The slope of the best fit line (Figure 8) gave a conversion factor of 132.3 pixels/Volt.

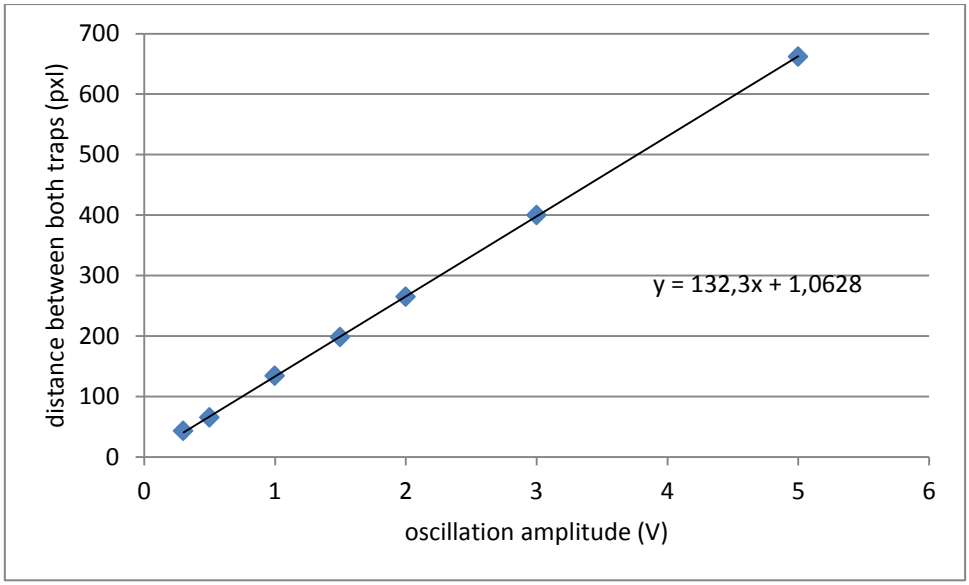

Figure 8: calibration curve for voltage given to the AOD and the corresponding beam position displacement at the sample level, this data above is only for the y-direction calibration

The second step was producing another calibration curve to convert screen pixels to actual displacements in micrometers. This was done by moving the piezo-stage in micrometer steps and observing the position displacement of the center of a silica particle stuck to the sample chamber bottom. The following calibration curve (Figure 9) was produced.

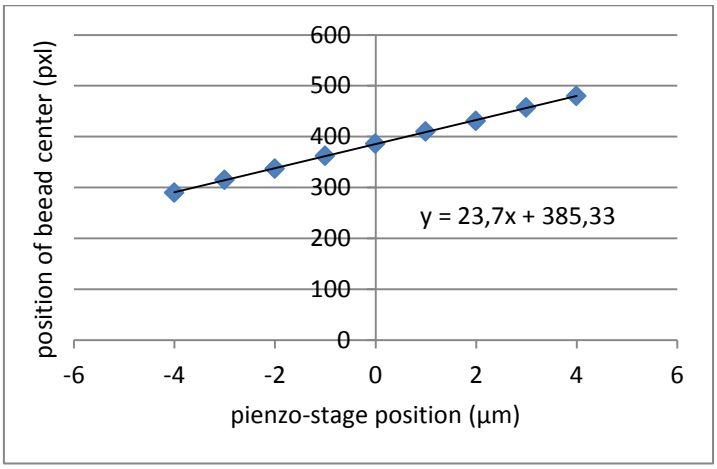

Figure 9: calibration curve for moving the sample in steps of micrometers and the corresponding beam position in pixels, this data above is only foe y-direction calibration

The resulting conversion factor was 23.7 pixels /micrometer. Using the two obtained factors, we get the micrometer-to-VAOD conversion factor for the setup. It was equal to 5.58228 µm/Volt.

For each trapped particle, the relation between the AOD and QPD voltages had to be measured. The "wiggling" technique was applied using a voltage controlled oscillator (VCO) to control the AODs. A 5 kHz triangular waveform was fed to the VCO using a function generator. The function generator operated in gate-mode and produced the wave only for 1 millisecond every 99 milliseconds. Figure 10 below shows a schematic representation of this oscillation.

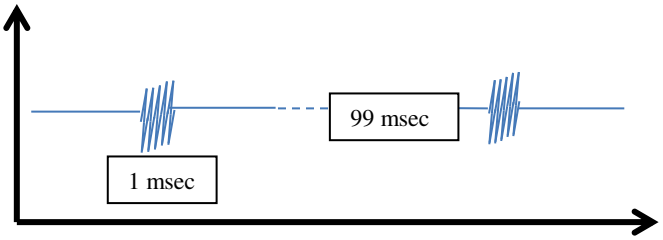

Figure 10: a schematic description for the voltage signal used at the input of the AOD

Each 1 ms signal caused 12 rapid complete sweeps over the trapped particle (five full waves starting at the center of the particle). The intensity profile was recorded using the QPD. The same procedure was repeated without the particle producing another data set to be used to correct the original set for background effects. A conversion factor between V_{AOD} and V_{QPD} was obtained. Combining the above calibration factors provided a conversion factor between the QPD voltage and the position of the particle in the sample in meters.

(3) Sample Preparation

The preparation of **worm-like micelles** was done following the procedure in (Buchanan, et al. 2005).

The ingredients[3] used were:

- cetylpyridinium chloride (CPyCl) - used as the surfactant
- sodium chloride (NaCl) - to make brine
- sodium salicylate (NaSal) - to be the strongly binding counterion

[3] All chemicals were obtained from Sigma Chemical Co. (Sigma-Aldrich Chemie B.V. Zwijndrecht, The Netherlands).

- de-ionized (DI) water (H_2O)

The process was as follows:

- Brine was prepared as a 0.5 M NaCl solution in DI water
- CPyCl and NaSal were dissolved in it such that the molar ratio of Sal/CPy is 0.5
- different concentrations (0.5, 1, 2, 3, 4 wt%) were prepared in patches of 25 mL
- patches were then stored inside a 27 °C incubator (above the system's Krafft point)
- a small amount, of silica particles[4] with a diameter of 0.936 µm was added to each sample right before each measurement (such that particle concentration is 1 µg/ml)
- micelles experiments in this work used the 2 wt% concentration solution.
- measurements were done at a controlled room temperature of 21.4 °C (also above system's Krafft point)

Water samples were prepared using de-ionized water with the same silica particle concentration used in micelles. However, experiments in water were done using two silica particle sizes. One set of measurements used 0.936 µm and another used 0.608 µm particles. In all cases the concentration of silica particles was very small i.e. 1 µg/ml. This concentration was suitable because it meant that only one particle would be seen within about a 50x50 µm range in the field of view.

(4) Data Collection & Analysis

The voltage signal from the quadrant photodiode was calibrated to position data as described previously. The particle position data in the form of a time series was used to calculate the Power Spectral Density (PSD) via a process of Fourier transform (Mizuno, et al. 2008). The PSD shows how the variance of the position fluctuation data is contributed to by each frequency component of the recorded signal.

[4] Kisker Biotech GmbH & Co. KG, Steinfurt, Germany - size values are given for particle diameter

$$S(\omega) = \int_{-\infty}^{\infty} < u(t)u(0) > e^{i\omega t}\, dt. \qquad (16)$$

The fluctuation dissipation theorem (FDT) relates the linear response of a system to the fluctuations of the system in its equilibrium state (Kubo 1966). This fact is paramount to research in passive microrheology because it is used to relate the PSD data obtained from the QPD measurements to the complex response function of the system under investigation, $A(\omega)$, where

$$A(\omega) = A'(\omega) + i\, A''(\omega). \qquad (17)$$

PSD data is used to calculate the imaginary part of this function using,

$$A''(\omega) = \frac{\omega}{2\, k_B T}\, S(\omega) \qquad (18)$$

Once the imaginary part is obtained, given that measurements were done for a wide range of frequencies, the Kramers-Krönig integral can be used to evaluate the real part (Mizuno, et al. 2008).

$$A'(\omega) = \frac{2}{\pi}\, P \int_0^{\infty} \frac{\xi\, A''(\xi)}{\xi^2 - \omega^2}\, d\xi \qquad (19)$$

where P is the principal-value integral, which according to (Gittes, et al. 1997) should be computed on a discrete data set as a sine transform of $A''(\omega)$ followed by a cosine transform. As mentioned previously, the response measured this way is the apparent response of the system that includes the effect of the optical trap. The real response of the solution is obtained as discussed previously by measuring the response of the system at two laser powers. The shear modulus of the solution is obtained using the Stokes Einstein relation Equation-5

A custom-written MATLAB program (Appendix #1) was used to evaluate (β) and (ϕ) with the inputs being:

1. time series data of QPD recordings
2. displacement calibration factors calculated using the technique in the next section
3. Then the program uses (β) and (ϕ) along with the inputs:
4. trapped particle radius (r)
5. power factor (a)

The program output is the complex shear modulus G which is the main parameter of interest. It is to be noted that only data from the y-direction are presented in this research because of a systematic error detected in the x-direction data.

Eighteen complete data sets were collected, with each set including two files of 4 million data points each (sampled at 20 kHz) as the main measurements at low and high power. Each set also includes 8 files of 100,000 data points each (sampled 195 kHz) used for calibration purposes. File sizes range between 4 and 23 MB.

VI. Results & Discussion

As mentioned before, the experiments were performed in two media. The first one was water. Due to its known zero elasticity, the objective was to take two measurements at two different powers (using the same trapped particle) and use the responses from both of them (as per Equation-15) to calculate the elastic response of the medium which should be zero. The other medium was a solution of worm-like micelles. It was chosen to be an example of a medium with both viscous and elastic components of shear modulus (of known elasticity from previous research) to confirm that the method works in media other than water.

(1) Measurements in Water

a. Two Powers using 0.936 µm silica Particles

Three measurements were done in this part using three different particles but all of the same size (0.936 µm). This size of trapped particle is widely used in experiments of microrheology.

At first, the PSD curves were looked at to make sure they look consistent with what is expected in a water medium. A Lorentzian shape for the PSD is predicted. The results (Figure 11 to Figure 13) came out as follows.

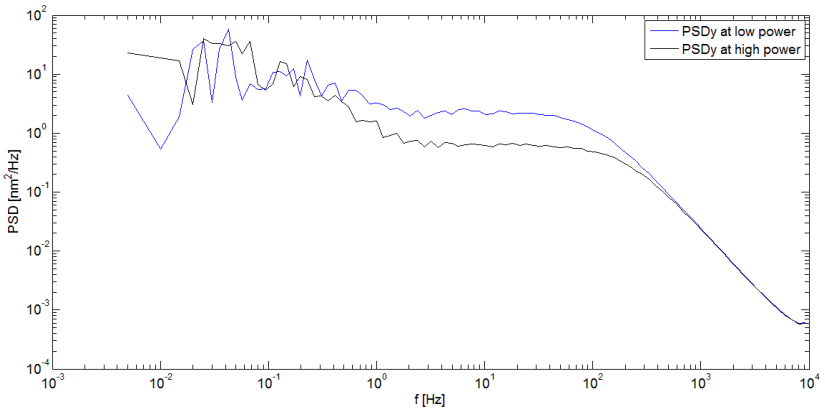

Figure 11: PSD curve for Sample 1 (particle size 0.936 µm - medium water)

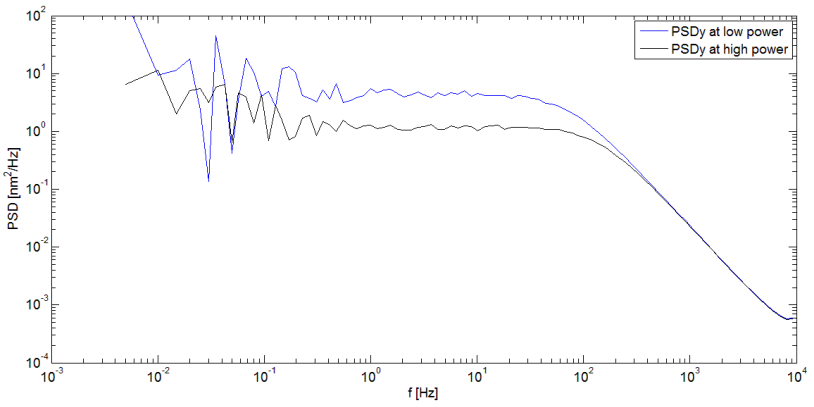

Figure 12: PSD curve for Sample 2 (particle size 0.936 µm - medium water)

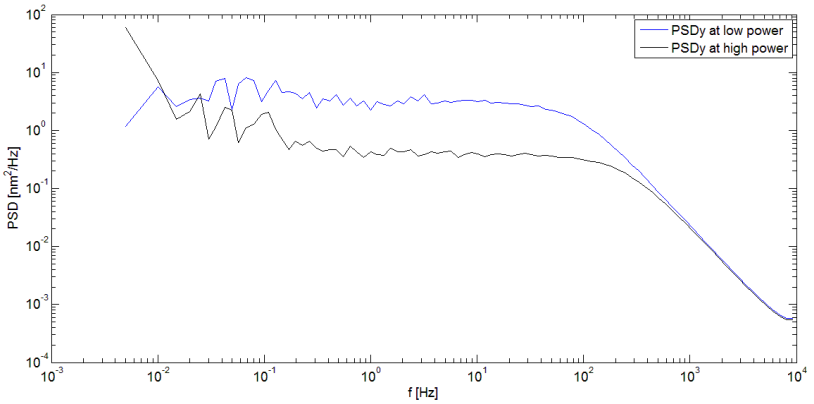

Figure 13: PSD curve for Sample 3 (particle size 0.936 µm - medium water)

At low frequencies, the effect of the trap in the PSD is clear. The larger the trap stiffness, the lower the PSD curve is. At very short times (high frequencies), the PSD is probing the properties of the solution which includes the viscosity and temperature. That is why the PSD curves for different powers are expected to overlap at high frequencies for data taken in the same medium.

Following the sequence explained in the data analysis section above, the response recorded at the two laser powers was used to eventually calculate the shear modulus of the medium. Although the shear modulus includes two components (elastic and viscous), only the real part of the modulus (elastic) is of concern here. This is because the effect of the laser trap is to add an apparent elastic component only to the complex shear modulus.

Figure 14 to Figure 16 below show the real part of the shear modulus (G') as a function of frequency.

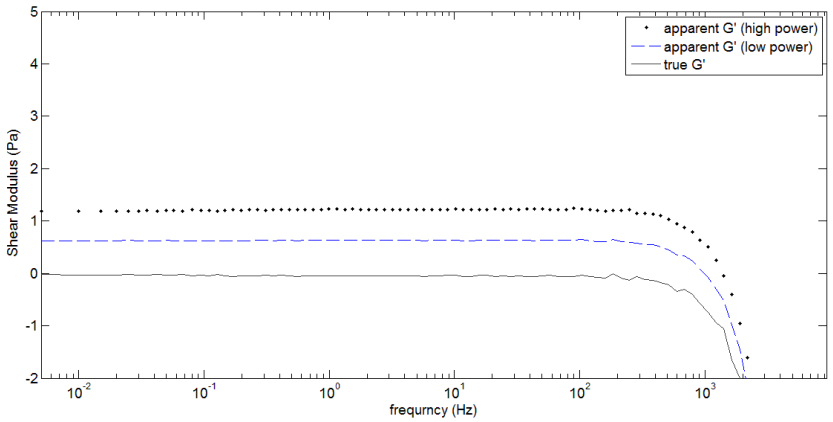

Figure 14: G' for Sample 1 (particle size 0.936 m - medium water)

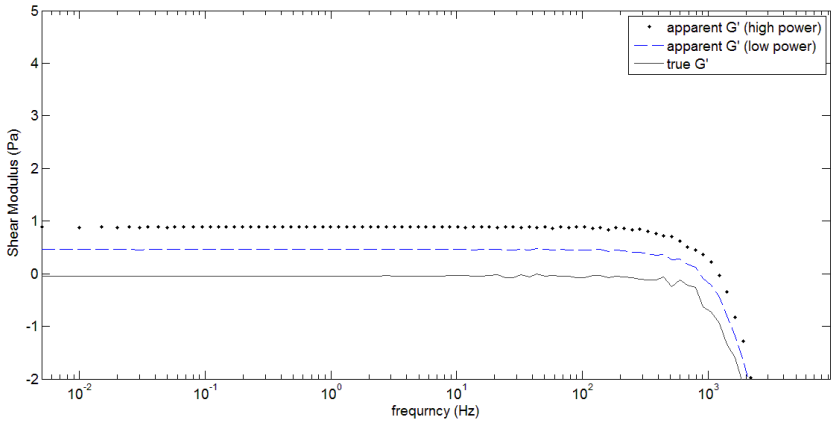

Figure 15: G' for Sample 2 (particle size 0.936 µm - medium water)

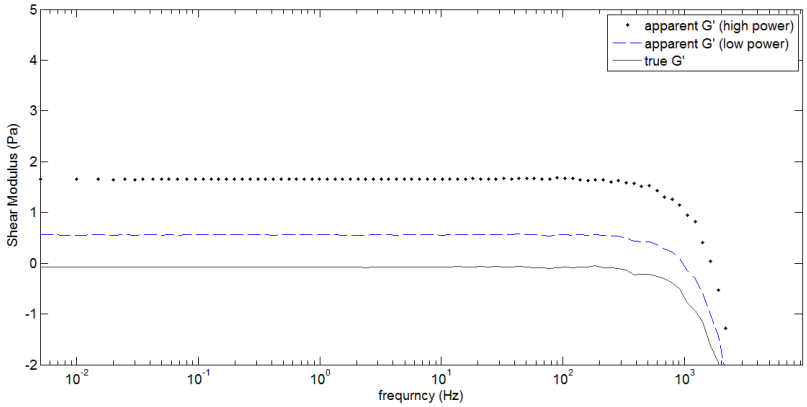

Figure 16: G' for Sample 3 (particle size 0.936 µm - medium water)

The results from Samples 1-3 are significant because they show that the new method proposed in this research is good at correcting the effect of a laser trap. Water should only have a viscous component of shear modulus.

The small deviations of the true elastic modulus from the expected zero result were regarded as resulting from experimental noise, especially that they are minor deviations if compared to the values of the elastic response at the two laser powers used. More research is needed to look into the exact causes of these deviations.

The turndown in the elastic shear modulus which starts to be evident at 200 Hz is due to the finite amount of data that was used to calculate the shear modulus. Any data above 200 Hz in Figure 14 to Figure 16 do not represent real properties of the solution (Schnurr, et al. 1997).

b. Two Powers using 0.608 µm silica Particles

For the three samples (Samples 4-6) with 0.608 µm particle size, the PSD curves appear as follows (Figure 17 to Figure 19).

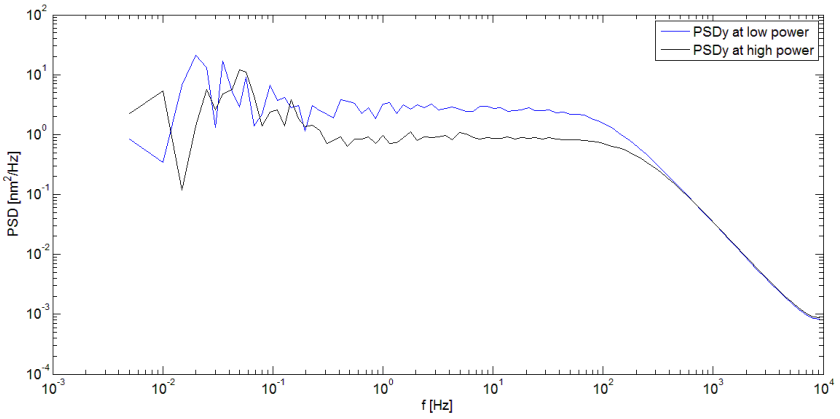

Figure 17: PSD curve for Sample 4 (particle size 0.608 µm - medium water)

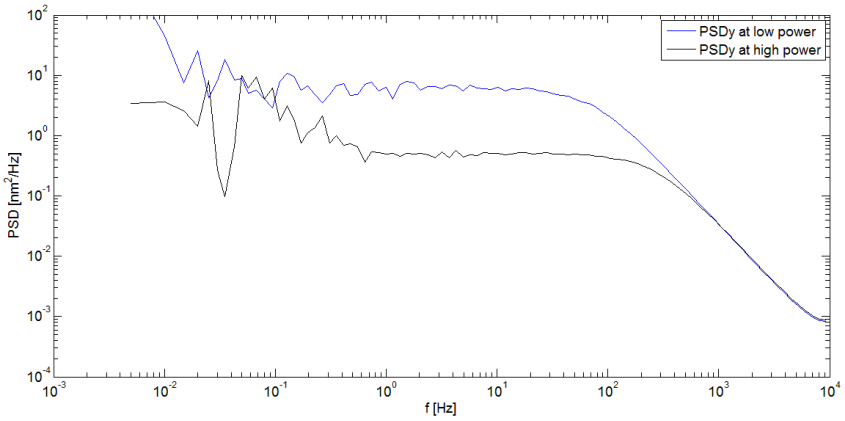

Figure 18: PSD curve for Sample 5 (particle size 0.608 µm - medium water)

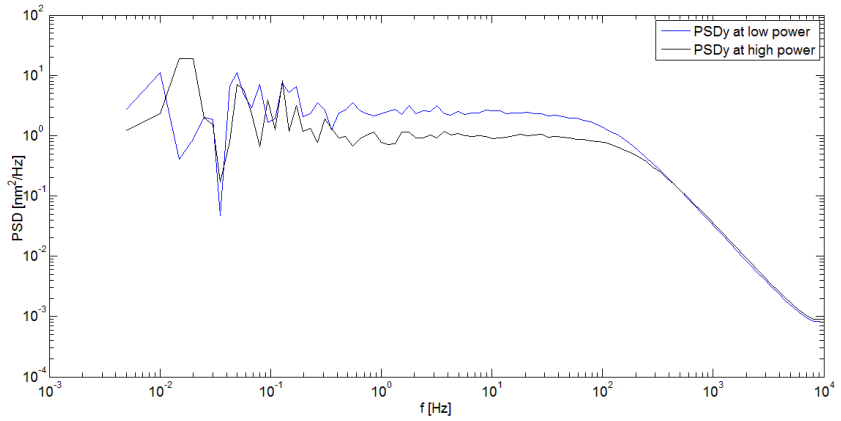

Figure 19: PSD curve for Sample 6 (particle size 0.608 µm - medium water)

The G'(ω) results also proved to agree with the expected zero shear modulus for water. Figure 20 to Figure 22 below show this.

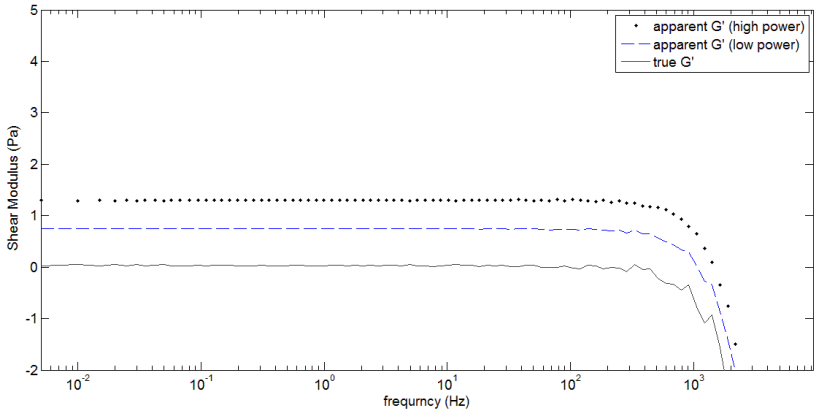

Figure 20: G' for Sample 4 (particle size 0.608 µm - medium water)

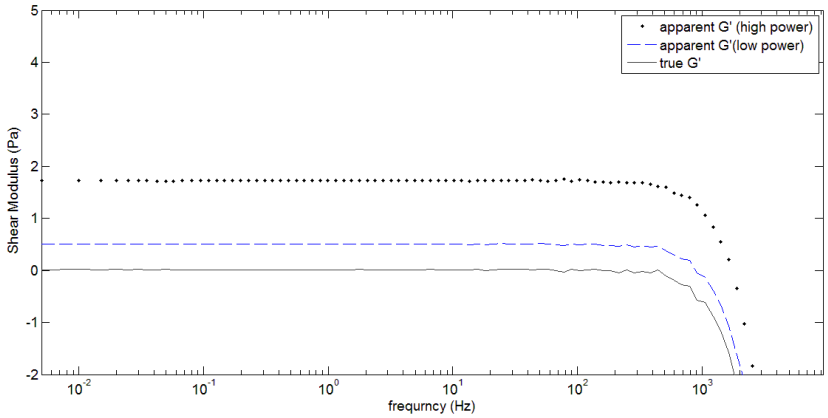

Figure 21: G' for Sample 5 (particle size 0.608 µm - medium water)

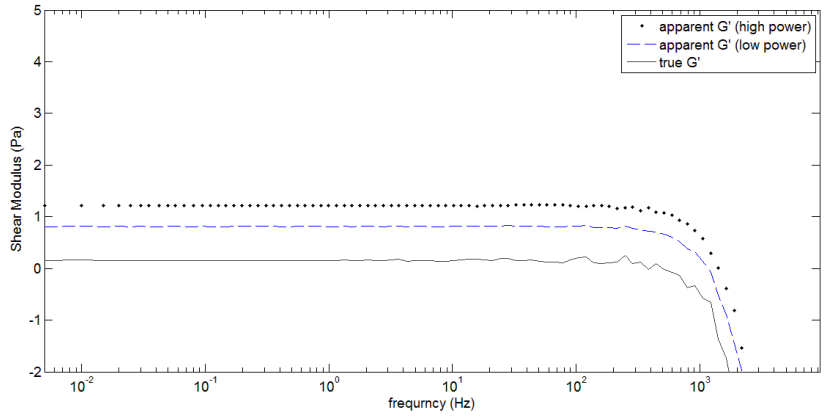

Figure 22: G' for Sample 6 (particle size 0.608 µm - medium water)

c. Generalization to Multiple Powers

The method of trap correction was extended to the case of multiple powers. This was done by measuring the elastic shear modulus at different laser powers for the same trapped particle. Figure 23 shows the apparent G' for four[5] of the five laser powers used (blue dashed lines). The elastic shear modulus increases as the laser power is increased as expected since the optical trap is stronger for higher powers.

To correct for the effect of the optical trap using many powers, the apparent G' was plotted as a function of laser power for each frequency. Figure 24 shows the plot of the apparent G' at five laser powers at 0.005 Hz. As expected, the apparent G' increases linearly with power. The y-intercept of the plot 0.0325

[5] the fifth was omitted from the graph because it was too high compared to the others, which would have made them less visible

Pa corresponds to the value of G' at zero optical power which corresponds to the shear elastic modulus of the solution at that frequency. Making a linear fit of the apparent G' as a function of optical power at each frequency and obtaining the y-intercept gives the true solution elastic modulus for each frequency. The black line in Figure 23 represents the true elastic modulus of the solution obtained using the linear regression analysis.

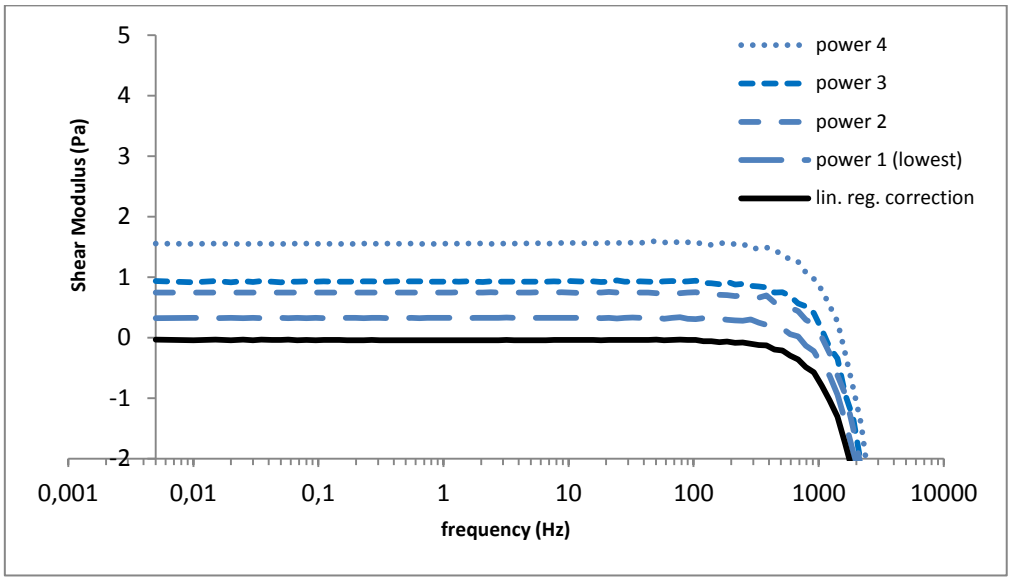

Figure 23: four of the five apparent G' measured at five different laser powers, in addition to the true G' corrected by linear regression of all five responses (particle size 0.936 - medium water)

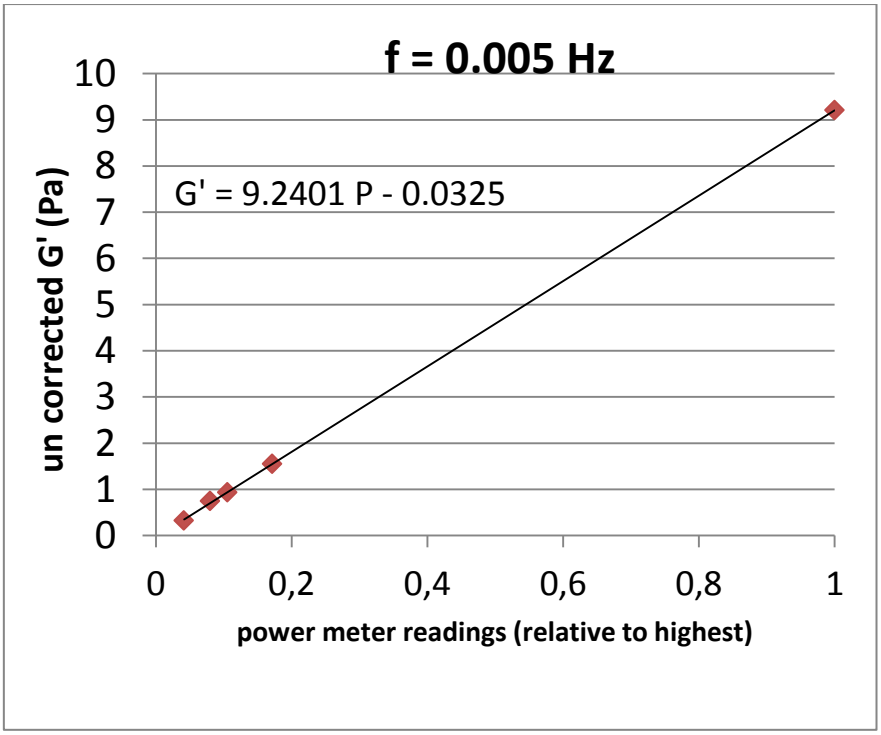

Figure 24: apparent G' at a given stress frequency for five different powers

The results from this group of measurements (although not very decisive in offering an exact way to optimize the method) open the door for big improvements to the method proposed here. They suggest that much study is needed to benchmark two variables (illustrated in Figure 25) for all types of microrheological experiments. These variables are:

1. the absolute value of stiffness from the lower laser power (h_{low})
2. the relative difference between the two powers used (d)

Understanding the effect of those two variables on the accuracy of the resulting trap correction will be very helpful in deciding which two laser powers to use in different media. It will also help researchers account for different limitation proposed by the experiment at hand (e.g. very high laser powers can be damaging to some biological samples).

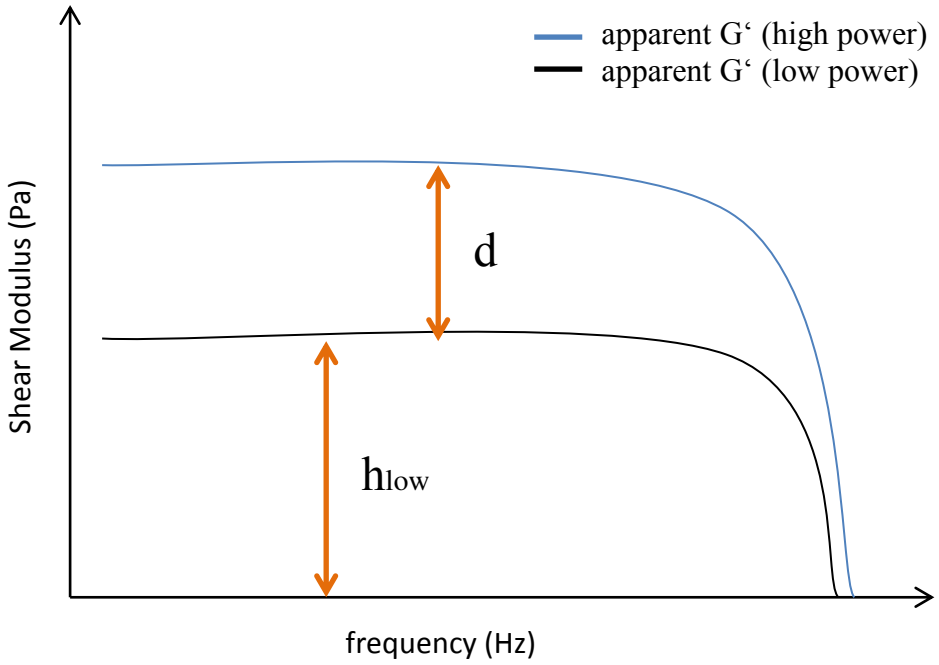

Figure 25: schematic diagram to illustrate the two parameters d & h_{low}

The data set including response from all five laser powers was utilized in a different way. That is, using each pair as a set to calculate the complex shear modulus by solving Equation-15. The results from this attempt are attached in Appendix #2 to help future researchers investigate the best combination of powers to use. Such research by definition would need several measurements using different combinations of laser powers. The best pair of laser powers to conduct measurements would be determined based on how accurate it predicts the previously-know G' of the medium under study.

It is important to note though, that taking measurements at more than two laser powers for the same particle can be experimentally very tricky. Unlike with the two power case (where the particle only needs to be trapped once to complete all the necessary recordings), this includes trapping and un-trapping the particle several times. It is due to the need to record the background signal before changing the laser power. This problem with many-power measurements can cause the loss of the trapped particle in the middle of the process (which implies repeating the whole measurement all over again).

(2) Measurements in Wormlike Micelles

a. Two Powers using 0.936 µm silica Particles

It appears so far that the results from measurements in water prove the point of this research. That is, using the medium response at two different laser powers to eliminate the effect of the optical trap. However, it was important to check the applicability of this method for a solution that has an elastic component to the shear modulus. Using 0.936 µm particles, the 2 wt% solution of worm-like micelles was the medium used for this test. The G' graphs for Samples 10-12 appear as follows (Figure 26 to Figure 28).

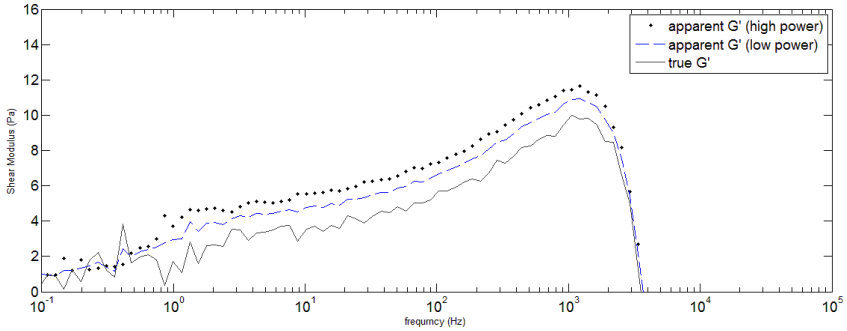

Figure 26: G' for Sample 7 (particle size 0.936 µm - medium WLM)

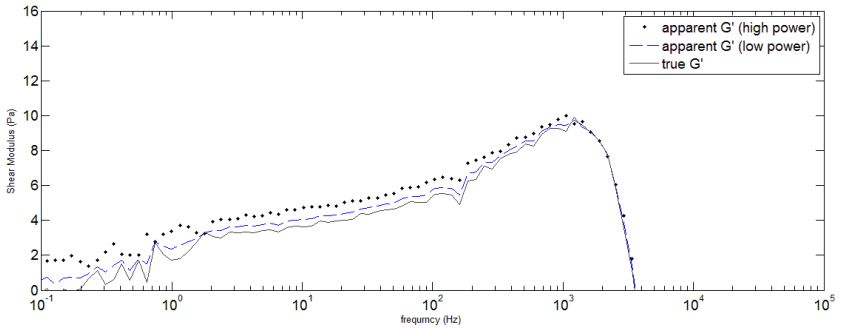

Figure 27: G' for Sample 8 (particle size 0.936 µm - medium WLM)

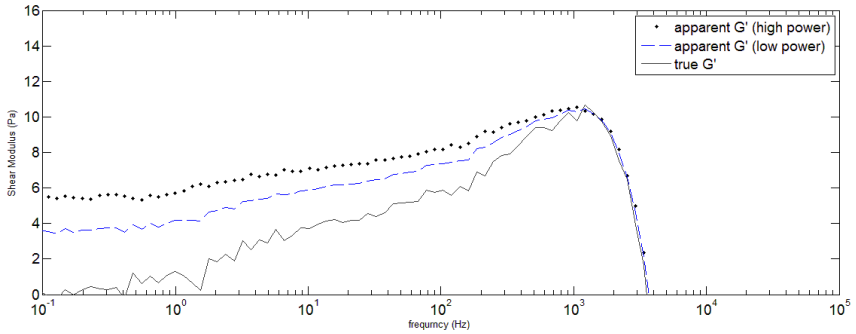

Figure 28: G' for Sample 9 (particle size 0.936 µm- medium WLM)

The G'(ω) detected in worm-like micelles in different samples show the same pattern (Figure 29) of rising from around 2 to 10 Pa between frequencies 1-1000 Hz. This result agrees with the measured elastic shear modulus in FIG-3 of (Buchanan, et al. 2005) for the same range of frequency and the same concentration of wormlike micelles, which is 2 wt%.

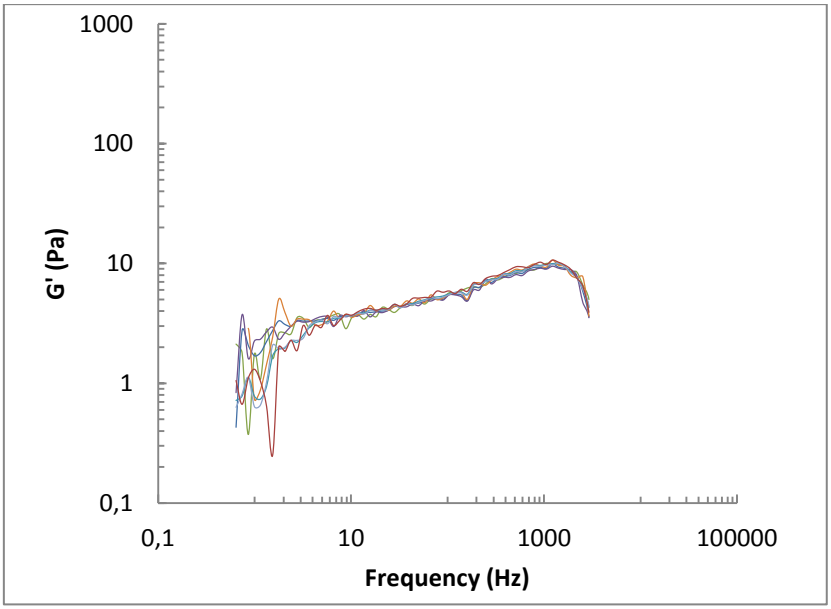

Figure 29: a collection of all G' curves calculated in the research for this thesis

b. Generalization to Multiple Powers

The generalization by using multiple powers instead of just two was done in wormlike micelles too. However, it was tried using only 3 different laser powers (seen in color in Figure 31). To correct for the effect of the optical trap using many powers, the apparent G' was plotted as a function of laser power for each frequency. Figure 32 shows the plot of the apparent G' at 3 laser powers at 50.3 Hz.

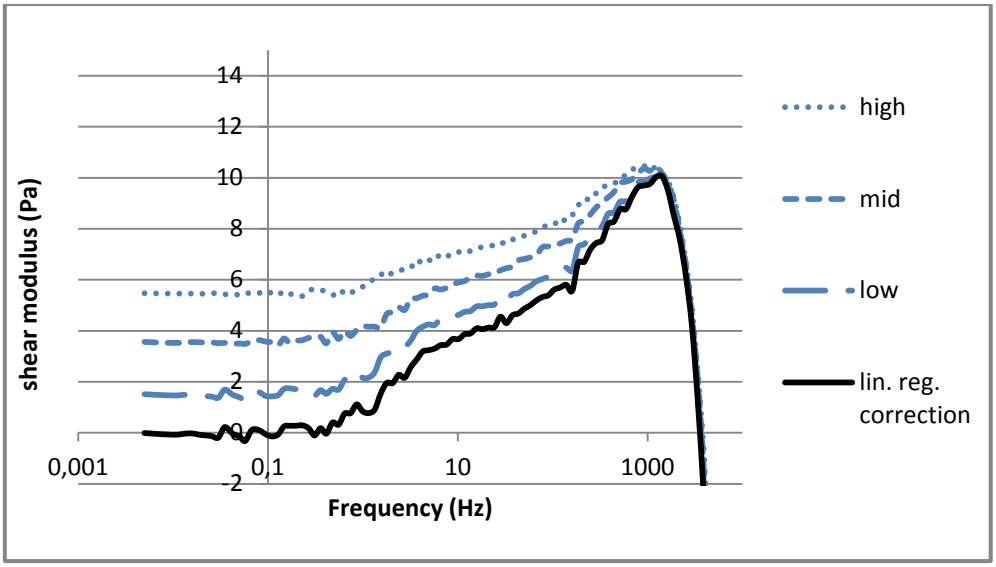

Figure 30: linear regression result in wormlike micelles solution

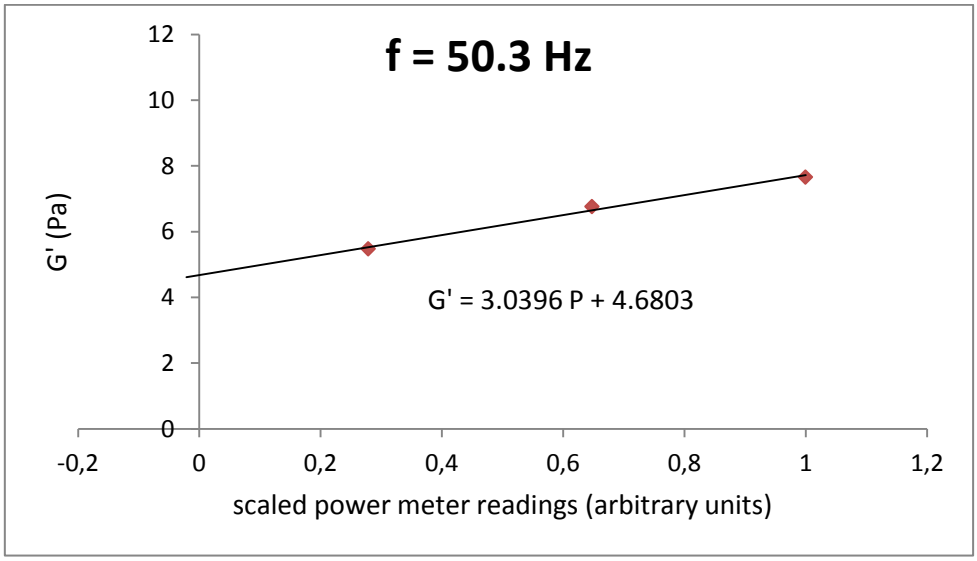

Figure 31: one example of the 92 linear fits used to calculate G' of wormlike micelles using 3 laser powers

As expected, the apparent G' increases linearly with power. The y-intercept of the plot 4.6803 Pa corresponds to the value of G' at zero optical power which corresponds to the shear elastic modulus of the solution at that frequency. Making a linear fit of the apparent G' as a function of optical power at each frequency and obtaining the y-intercept gives the true solution elastic modulus for each frequency. The black line in Figure 31 represents the true elastic modulus of the solution obtained using the linear regression analysis.

Figure 33 below shows that the results from linear regression are not so different from those obtained by doing the correction using each two powers together.

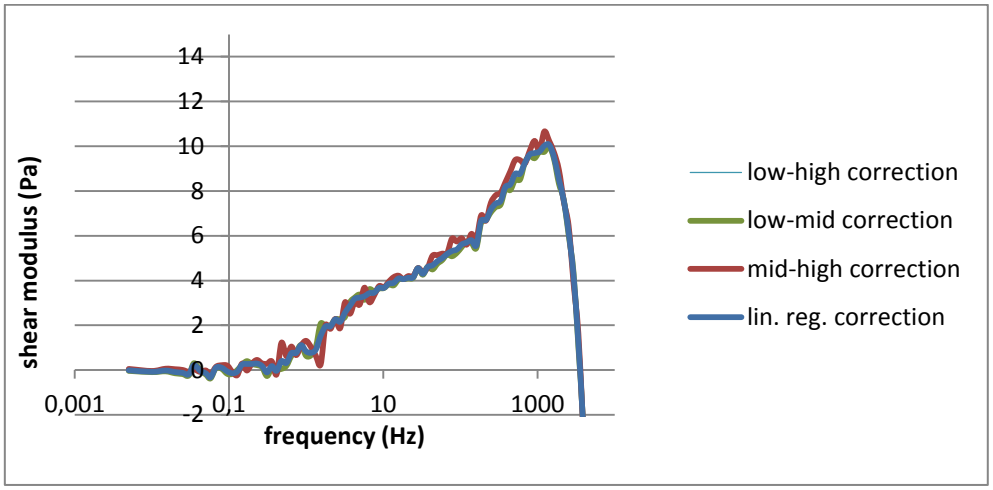

Figure 32: similarity in the results from two-power corrections and linear regression correction using all three powers

VII. Conclusion & Future Outlook

Using optical traps in studying microrheology always requires a correction process to remove the contribution of the trap to the elastic part of the measured medium response. Several experimental methods are available to correct for this effect. A new method is proposed in this research. It is based on taking measurements at two different laser powers then using both responses to obtain the true medium response. It was found to be an effective method to account for the optical trap stiffness in microrheological experiments. It requires less labor and avoids possible sources of error involved in the traditional methods of repeating the experiment in separate samples of purely-viscous media using different trapped particles.

In addition to testing the effectiveness of the method, it has been tested in a solution of worm-like micelles to check its viability in solutions that have a non-zero elastic shear modulus. Measurements in water yielded a zero elastic shear modulus as predicted, and those in micelle solution yielded results that were in agreement with previously published data for micelle solutions.

The method of trap correction was generalized to the case of multiple powers. Choosing different pairs of laser powers in this experiment gave good results but more investigation is required to tackle two important considerations. The first is how low the lower power should be (to avoid noise signal interference if the trap is very weak). Second, what should the relative difference between the two trap powers be? Future research in this area can maximize the benefits of this new two-power method. It can also provide insight on the possible combinations of laser powers to be used in samples sensitive to high powers (e.g. cells).

VIII. References

Addas, Karim M., Christoph F. Schmidt, and Jay X. Tang. "Microrheology of solutions of semiflexible biopolymer filaments using laser tweezers interferometry." *PHYSICAL REVIEW E* 70 (2004): 021503.

Ashkin, A. "Forces of a single-beam gradient laser trap on a dielectric sphere." *Biophysical Journal* 61 (1992): 569-582.

Ashkin, A., J. M. Dziedzic, J. E. Bjorkholm, and Steven Chu. "Observation of a single-beam gradient force optical trap for." *OPTICS LETTERS* 11, no. 5 (1986): 288-290.

Buchanan, M., M. Atakhorrami, J. F. Palierne, F. C. MacKintosh, and C. F. Schmidt. "High-frequency microrheology of wormlike micelles." *PHYSICAL REVIEW E* 72 (2005): 011504.

Gittes, F., B. Schnurr, P.D. Olmsted, F.C. MacKintosh, and C.F. Schmidt. "Microscopic Viscoelasticity: Shear Moduli of Soft Materials." *Physical Review Letters , – Published 27 October 1997* 79, no. 17 (1997): 3286-3289.

Kubo, R. "The fluctuation-dissipation theorem." *Reports on Progress in Physics* 29 (1966): 255-284.

MacKintosh, F.C., and C.F. Schmidt. "Microrheology." *Current Opinion in Colloid & Interface Science* 4 (1999): 300-307.

Marti, Othmar, and Katrin Hübner. "Force Measurements with Optical Tweezers." Chap. D.32 in *Handbook of Nanotechnology*, edited by B. Bhushan, 1013-1022. Heidelberg: Springer Verlag, 2010.

Mizuno, D., D. A. Head, F. C. MacKintosh, and C. F. Schmidt. "Active and Passive Microrheology in Equilibrium and Nonequilibrium Systems." *Macromolecules* 41, no. 19 (2008): 7194-7202.

Neuman, Keir C., and Steven M. Block. "Optical trapping." *Review of Scientific Instruments* 75, no. 9 (2004): 2787-2809.

Schnurr, B., F. Gittes, F. C. MacKintosh, and C. F. Schmidt. "Determining Microscopic Viscoelasticity in Flexible and Semiflexible Polymer Networks from Thermal Fluctuations." *Macromolecules* 30 (1997): 7781-7792.

Smith, S B., Yuija Cui, and Carlos Bustamante. "Optical-Trap Force Transducer That Operates by Direct Measurement of Light Momentum." *METHODS IN ENZYMOLOGY* 361 (2003): 134-162.

Vermeulen, Karen C., Joost van Mamerena, Ger J. M. Stienen, Erwin J. G. Peterman, Gijs J. L. Wuite, and Christoph F. Schmidt. "Calibrating bead displacements in optical tweezers." *Review of Scientific Instruments* 77 (2006): 013704.

Viana, N. B., M. S. Rocha, O. N. Mesquita, A. Mazolli, P. A. Maia Neto, and H. M. Nussenzveig. "Towards absolute calibration of optical tweezers." *PHYSICAL REVIEW E* 75 (2007): 021914.

IX. Appendices

(1) Appendix #1: Matlab® Code

A computational package "MRToolbox-v3.3-2nov-2012" was developed in the lab of Prof. Christoph Schmidt to analyze the data and obtain the response and shear modulus of the solution as outlined in the data analysis section.

The following function was developed for the purpose of applying the new technique proposed in this research. It takes as its inputs the uncorrected G' (both at high and low laser powers) calculated using the above-mentioned package. It takes as input the parameter ‘’a’’. The function also requires the radius of the trapped particle as an input.

Main Function used to apply Equation-15

```
a = input('Specify the value of a ... ');
R = input('Specify particle diameter in [nm] ... ') * 1e-9 / 2;
 % get the uncorrected-for-trap moduli
Gx_uncorr_low = low{1,1}.Gx_uncorr;
Gx_uncorr_high = high{1,1}.Gx_uncorr;
Gy_uncorr_low = low{1,1}.Gy_uncorr;
Gy_uncorr_high = high{1,1}.Gy_uncorr;


beta_x = low{1,1}.G.x.A_cal;
phi_x = high{1,1}.G.x.A_cal;
beta_y = low {1,1}.G.y.A_cal;
phi_y = high {1,1}.G.y.A_cal;


numerator_x = (beta_x)-(phi_x);
denominator_x = a.*(beta_x).*(phi_x);
numerator_y = (beta_y)-(phi_y);
denominator_y = a.*(beta_y).*(phi_y);
```

```
kx = real(numerator_x./denominator_x);

ky = real(numerator_y./denominator_y);


top_x = a.*(beta_x).*(phi_x);

down_x = (a+1).*(phi_x)-beta_x;

top_y = a.*(beta_y).*(phi_y);

down_y = (a+1).*(phi_y)-beta_y;


alpha_all_x = top_x./down_x;

alpha_all_y = top_y./down_y;

 %***********************************************

 % get the corrected moduli from the hi low method from the
full alpha

G_final_all_x = 1./(6*pi*R*alpha_all_x);

G_prime_all_x = real(G_final_all_x);

G_ddp_all_x = imag(G_final_all_x);


G_final_all_y = 1./(6*pi*R*alpha_all_y);

G_prime_all_y = real(G_final_all_y);

G_ddp_all_y = imag(G_final_all_y);

%***********************************************

 f1 = figure(1);


semilogx(high{1,1}.f,real(Gx_uncorr_high),'.',high{1,1}.f,real(
Gx_uncorr_low),'--',high{1,1}.f,G_prime_all_x)

axis([high{1,1}.f(1,1) high{1,1}.f(numel(high{1,1}.f),1) -2 5])

legend('apparent Gprime (high power)','apparent Gprime (low
power)', 'true Gprime')

title('G-x')

xlabel('frequrncy (Hz)')

ylabel('Shear Modulus (Pa)')
```

```
f2 = figure(2);


semilogx(high{1,1}.f,real(Gy_uncorr_high),'.',high{1,1}.f,real(
Gy_uncorr_low),'--',high{1,1}.f,G_prime_all_y)

axis([high{1,1}.f(1,1) high{1,1}.f(numel(high{1,1}.f),1) -2 5])

legend('apparent Gprime (high power)','apparent Gprime (low
power)', 'true Gprime')

title('G-y')

xlabel('frequrncy (Hz)')

ylabel('Shear Modulus (Pa)')
```

(2) Appendix #2: Data for Future Research

Below are the results from correcting for the trap stiffness using two apparent responses, trying all different combinations of five laser powers. The hypothesis here is that both the level of the low apparent G' as well as the difference between that at low power and that at high power affect how close the calculated true G' is to zero. All of these measurements were done using the same trapped particle (of size 0.936 μm) in a distilled water medium.

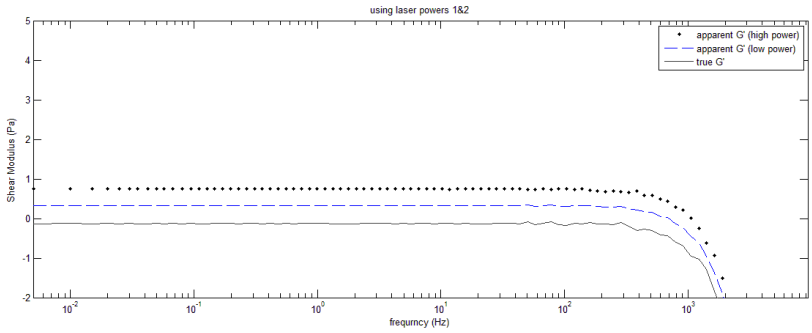

Figure 33: data for future research

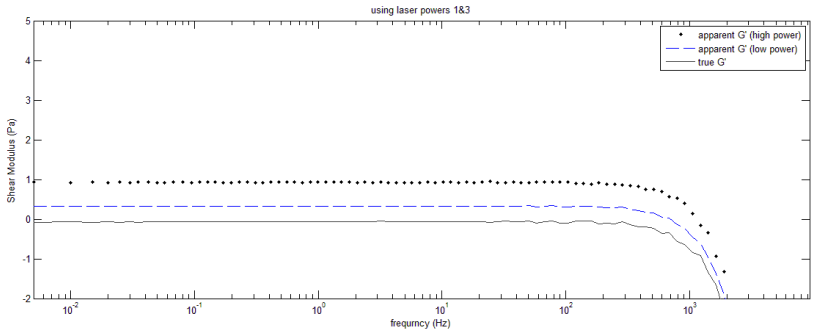

Figure 34: data for future research

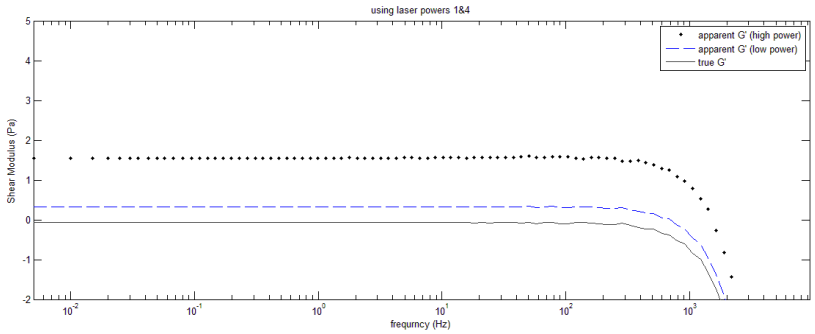

Figure 35: data for future research

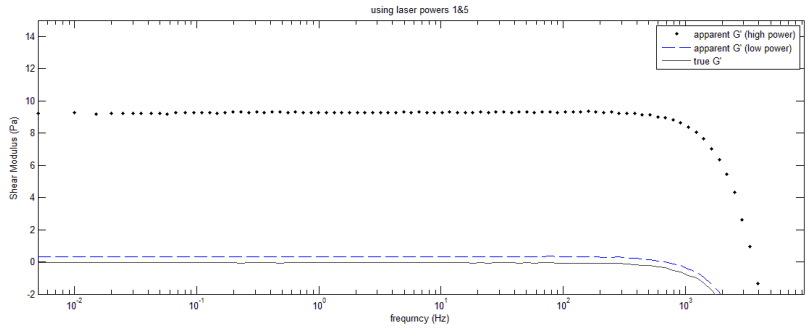

Figure 36: data for future research

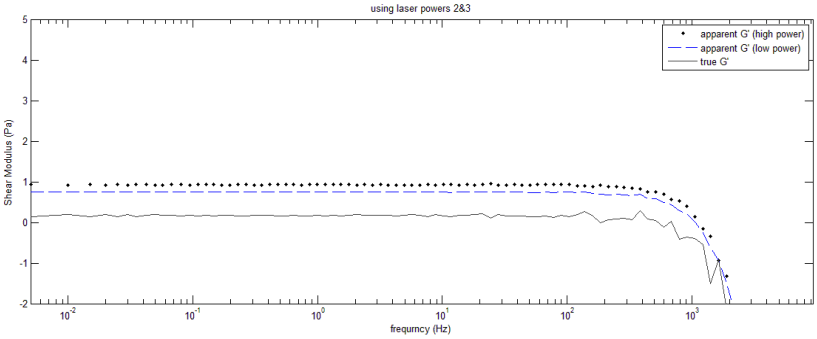

Figure 37: data for future research

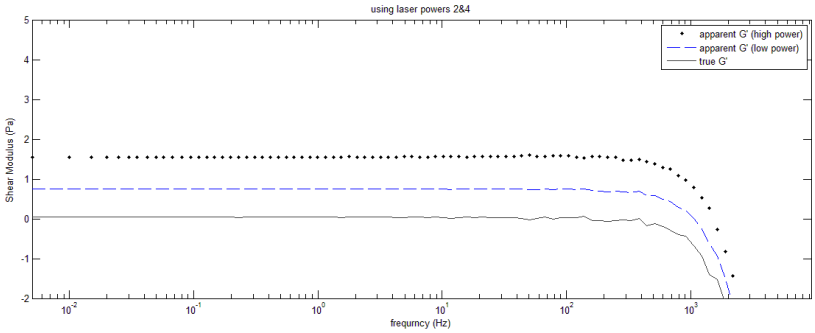

Figure 38: data for future research

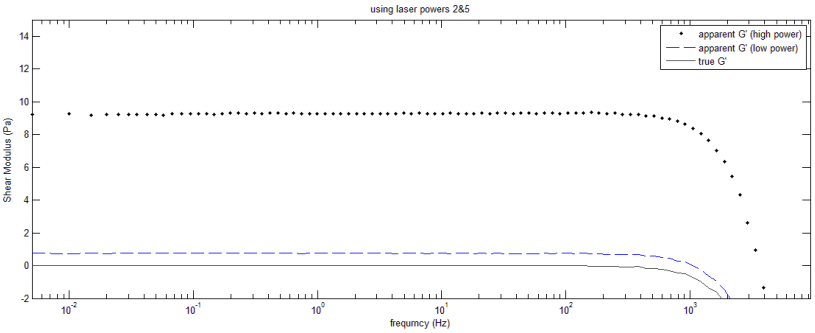

Figure 39: data for future research

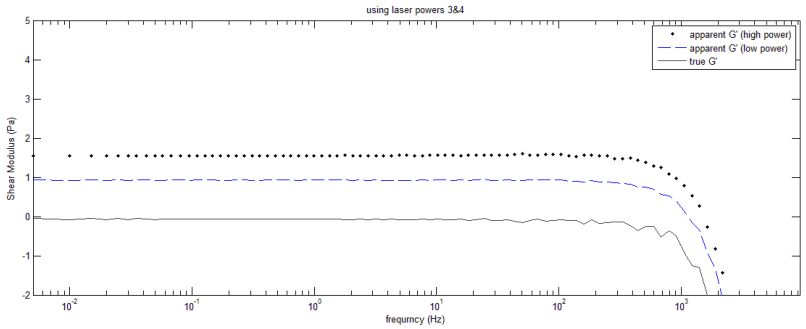

Figure 40: data for future research

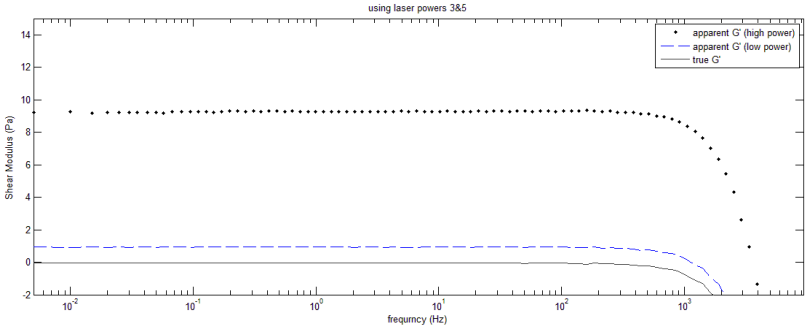

Figure 41: data for future research

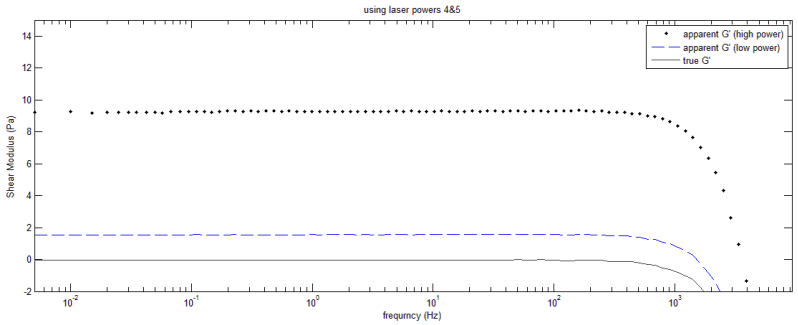

Figure 42: data for future research

(3) Appendix #3: Experimental Setup Pictures

In effort to introduce the used setup in a more familiar way, this appendix includes real pictures of the whole setup and some select setup components. All pictures were taken inside the lab in Göttingen University.

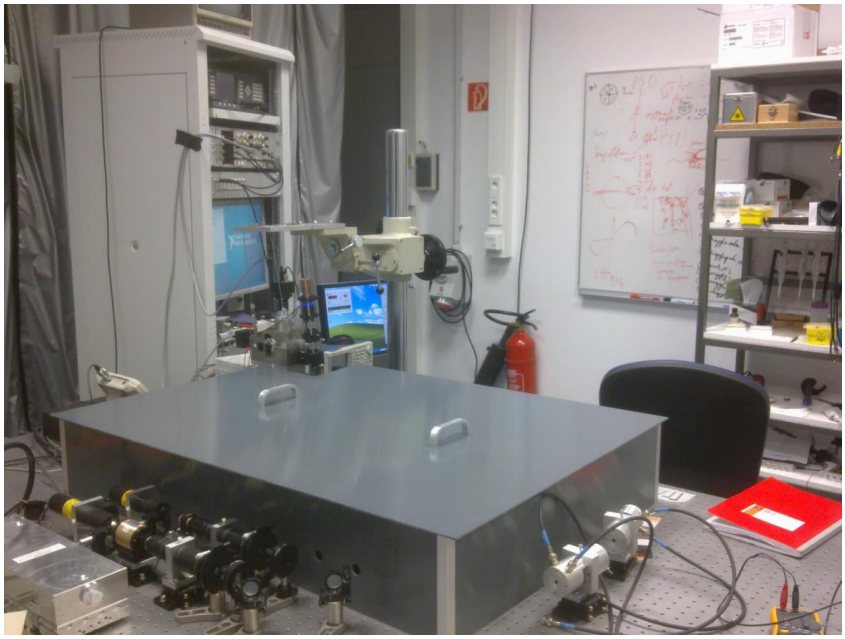

Figure 43: overview of the setup on the air table when it is covered to take measurements, the white stand behind on the left hold all the electronic equipment used (away from the table to reduce vibrations)

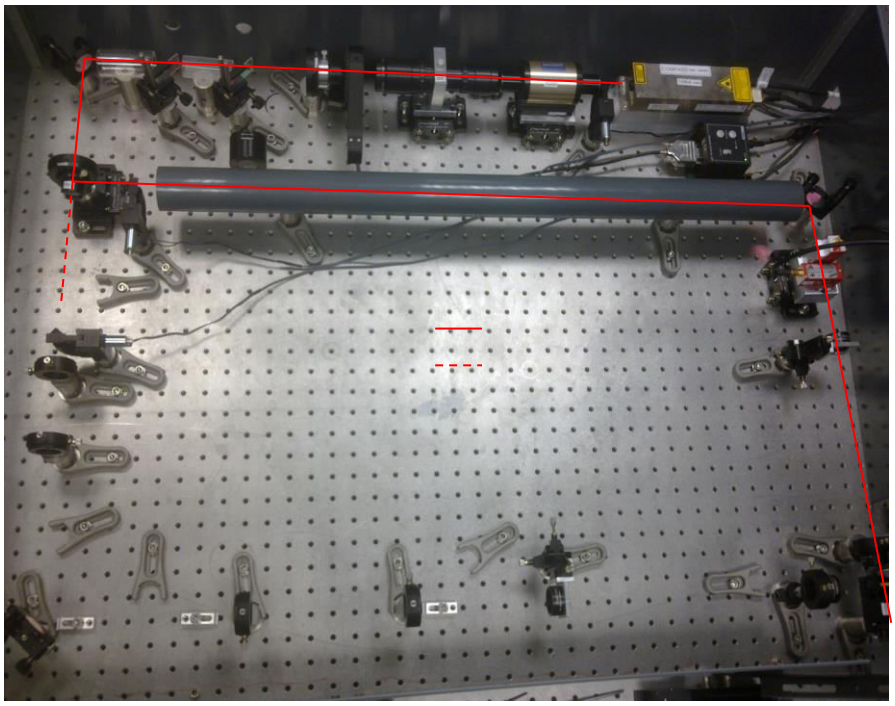

Figure 44: top view of the beam path before entering the microscope

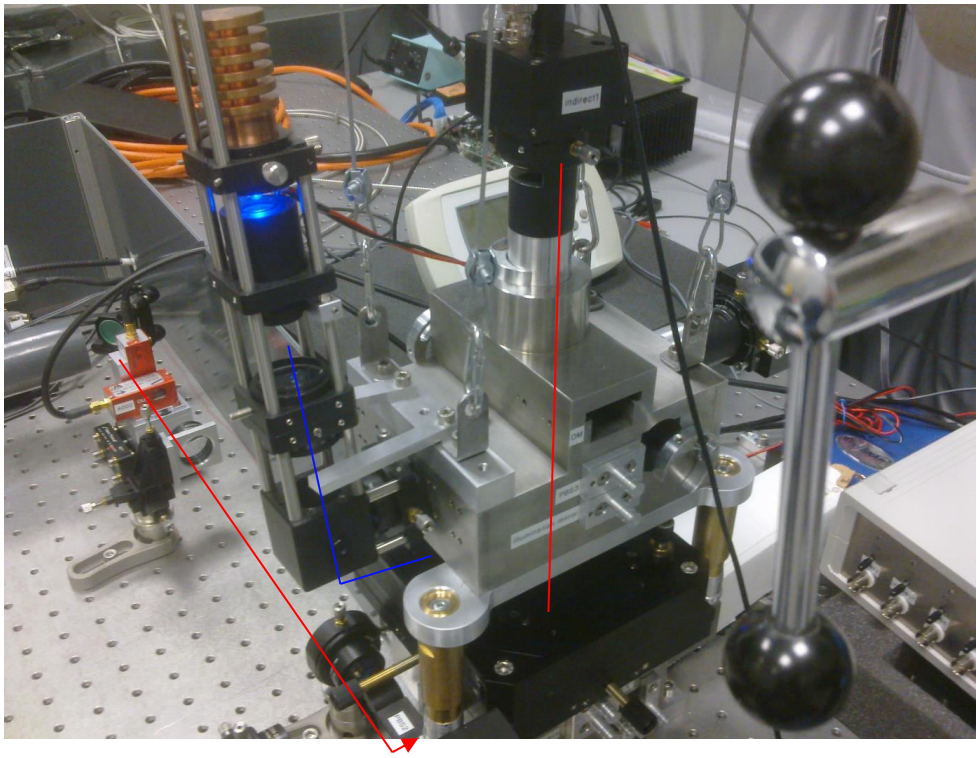

Figure 45: view of the chassis where the two objectives are placed into a vertical path starting at the sample and ending at the QPD

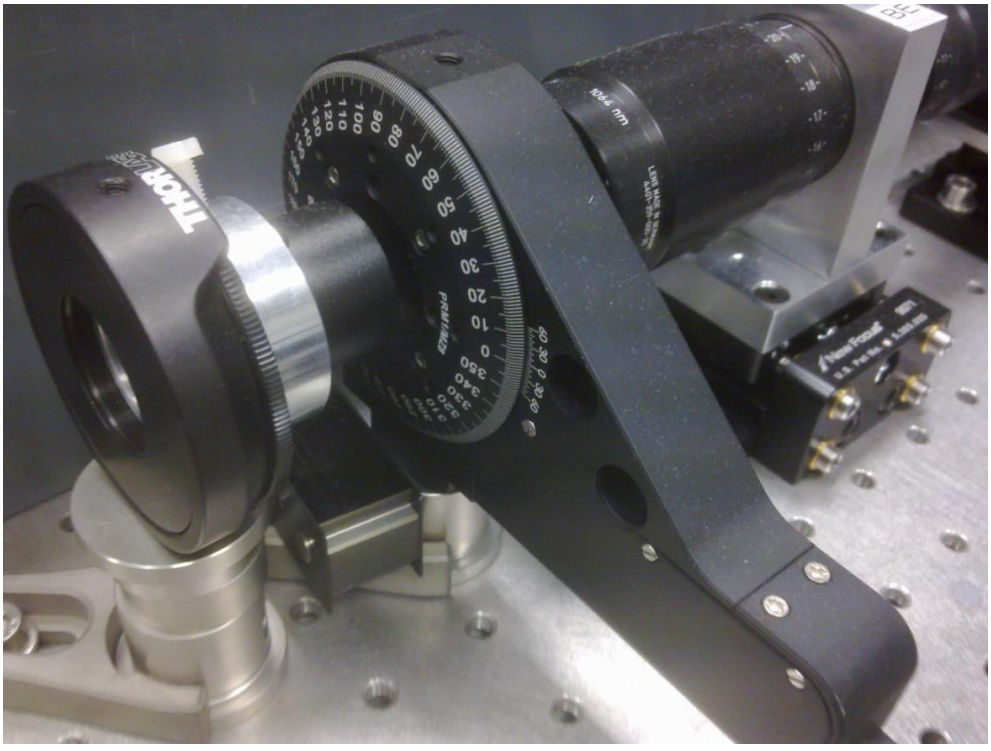

Figure 46: the combination of half-wave plate and Glanlaser polarizer used to change the laser power

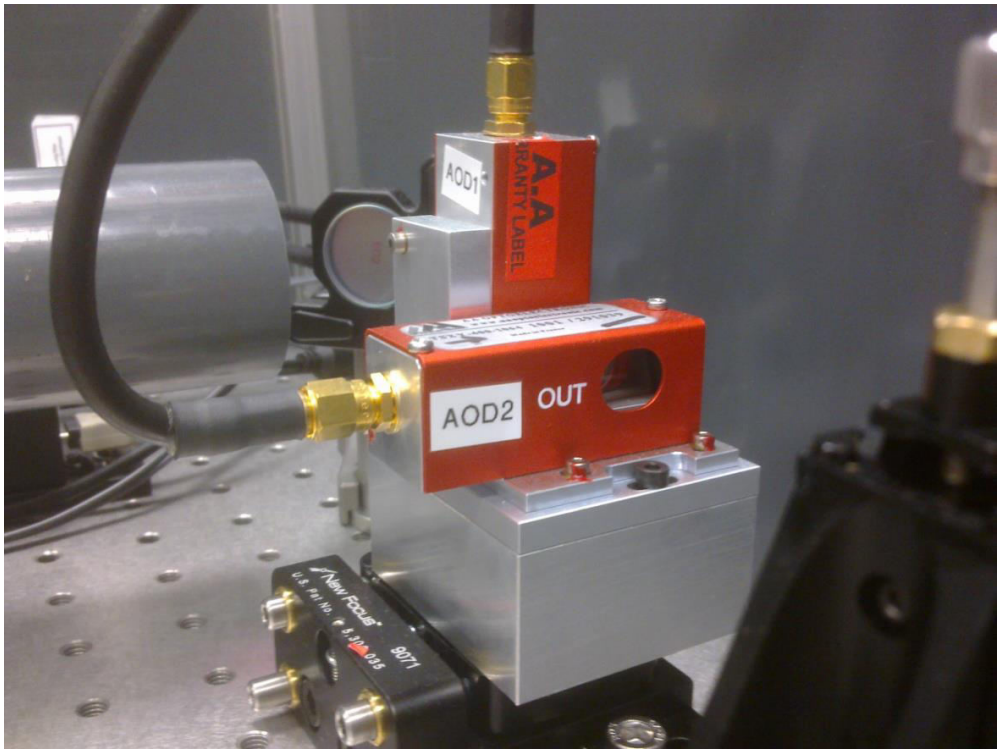

Figure 47: a pair of acousto-optic deflectors to steer the beam in both x and y directions

Figure 48: solutions of worm-like micelles with different concentrations prepared for this experiment and kept at constant temperature below their Kraft point

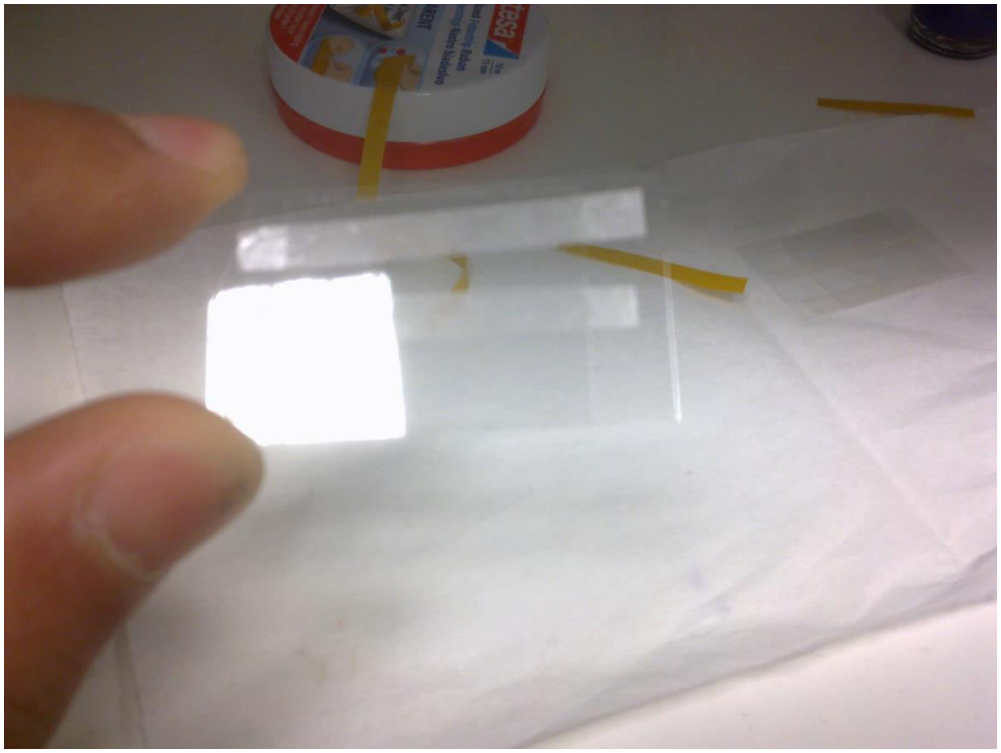

Figure 49: sample chamber before pipetting in the solution to be studied, double sticky tape is used to hold both glasses together, sealing (with nail polish) goes at the sides

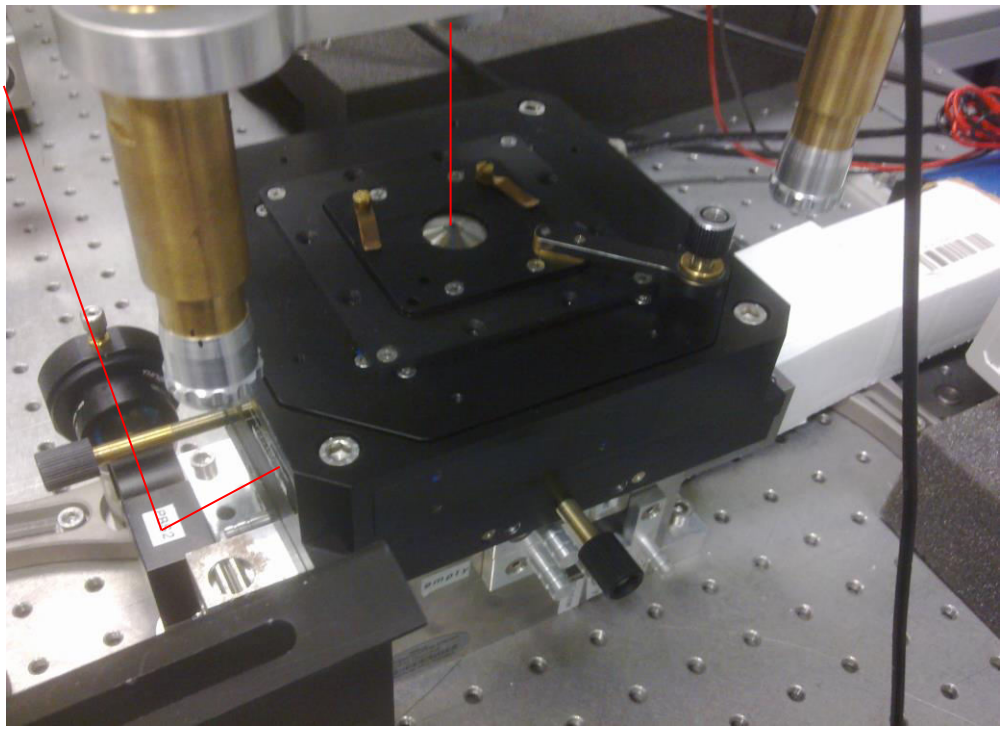

Figure 50: placing of the sample is done after lifting the upper part of the chassis resting on 3 legs

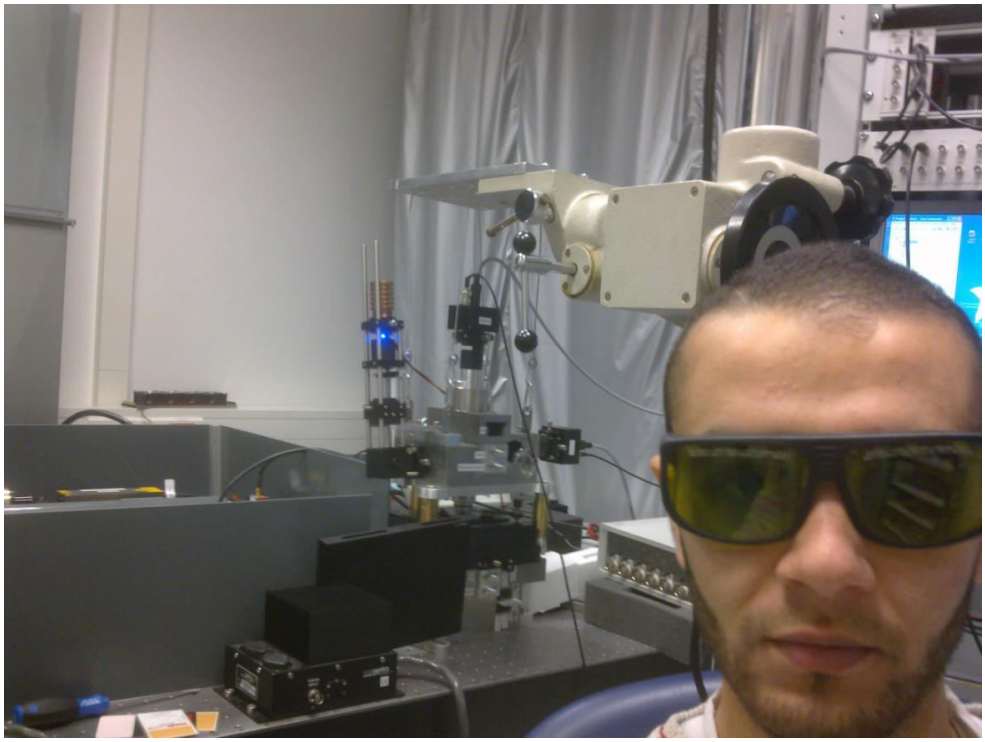

Figure 51: me in front of the setup putting on laser protection glasses necessary whenever the laser is on